SIMULTANEOUS RECORDING OF CALCIUM TRANSIENTS IN SKELETAL MUSCLE USING HIGH- AND LOW-AFFINITY CALCIUM INDICATORS

M. G. KLEIN, B. J. SIMON, G. SZUCS, AND M. F. SCHNEIDER

Department of Biological Chemistry, University of Maryland School of Medicine, Baltimore, Maryland 21201

ABSTRACT   To monitor cytosolic $[Ca^{2+}]$ over a wide range of concentrations in functioning skeletal muscle cells, we have used simultaneously the rapid but relatively low affinity calcium indicator antipyrylazo III (AP III) and the slower but higher affinity indicator fura-2 in single frog twitch fibers cut at both ends and voltage clamped with a double vaseline gap system. When both dyes were added to the end pool solution the cytosolic fura-2 concentration reached a steady level equal to the end pool concentration within ~2.5 h, a time when the AP III concentration was still increasing. For depolarizing pulses of increasing amplitude, the fura-2 fluorescence signal approached saturation when the simultaneously recorded AP III absorbance change was far from saturation. Comparison of simultaneously recorded fura-2 and AP III signals indicated that the mean values of the on and off rate constants for calcium binding to fura-2 in 18 muscle fibers were 1.49×10^8 $M^{-1}s^{-1}$ and 11.9 s^{-1}, respectively (mean $K_D = 89$ nM), if all AP III in the fiber is assumed to behave as in calibrating solution and to be in instantaneous equilibrium with $[Ca^{2+}]$. $[Ca^{2+}]$ transients calculated from the fura-2 signals using these rate constants were consistent with the $[Ca^{2+}]$ transients calculated from the AP III signals. Resting $[Ca^{2+}]$ or small changes in $[Ca^{2+}]$ which could not be reliably monitored with AP III could be monitored with fura-2 with little or no interference from changes in $[Mg^{2+}]$ or from intrinsic signals. The fura-2 signal was also less sensitive to movement artifacts than the AP III signal. After a $[Ca^{2+}]$ transient the fura-2 signal demonstrated a relatively small elevation of $[Ca^{2+}]$ that was maintained for many seconds.

INTRODUCTION

Calcium binding to relatively low affinity "calcium-specific" sites on thin filament troponin C (Zott and Potter, 1984) serves to activate contraction of skeletal muscle cells within milliseconds (Kress et al., 1986) of the large and rapid cytosolic calcium transient initiated by the muscle action potential (Miledi et al., 1977; Blinks et al., 1978; Baylor et al., 1982b). In contrast, small but prolonged depolarizations can increase muscle metabolism without producing any mechanical activation (Solandt, 1936; Smith and Solandt, 1938; Hill and Howarth, 1957). Such small depolarizations do produce small elevations in resting $[Ca^{2+}]$ (Lopez et al., 1983; Snowdowne, 1985), which could modulate intermediary metabolism in muscle via Ca^{2+} regulated enzyme systems (Malencik and Fischer, 1982). Selective activation of such metabolic systems could be achieved during small depolarizations if they were regulated by sites having a higher effective calcium affinity than thin filament troponin C.

In several previous studies from this laboratory we have used the metallochromic calcium indicator antipyrylazo

III (AP III) (Scarpa et al., 1978) to monitor calcium transients during voltage clamp depolarizations of skeletal muscle fibers. Analysis of such calcium transients has provided information regarding calcium release from the sarcoplasmic reticulum (SR) (Melzer et al., 1984, 1987; Melzer et al., 1986b), calcium depletion from the SR during release (Schneider et al., 1987a), possible $[Ca^{2+}]$-dependent inactivation of SR calcium release (Simon et al., 1985), and the properties of the systems involved in removing the released calcium from the myoplasm (Melzer et al., 1986a; Brum et al., 1987). However, the relatively low affinity of AP III (Rios and Schneider, 1981; Kovacs et al., 1983; Hollingworth et al., 1987) precludes its use to determine resting levels of $[Ca^{2+}]$. This was a serious limitation to some aspects of our studies, especially those characterizing the calcium removal systems. Furthermore, the small but prolonged elevations in calcium (Melzer et al., 1986a; Cannell, 1986) that follow the fast decline of the calcium transient after fiber repolarization are not monitored unambiguously with AP III because of the simultaneous occurrence of an often relatively large change in intrinsic transparency (Kovacs and Schneider, 1977; Baylor et al., 1982b; Melzer et al., 1986a) and the possibility of a component of the AP III signal due to changes in $[Mg^{2+}]$ (Baylor et al., 1985a, 1986).

To monitor [Ca^{2+}] accurately over the range of concentrations relevant to calcium regulation at both high- and low-affinity sites and to be able to monitor resting [Ca^{2+}] and small changes thereof, we have modified our previous apparatus to allow the simultaneous use of the rapid but relatively low affinity calcium indicator AP III and the slower but higher affinity calcium indicator fura-2 (Grynkiewicz et al., 1985). Fura-2 is a fluorescence indicator whereas AP III is an absorbance indicator and the wavelengths for fura-2 excitation and emission are well below the wavelengths that we use for monitoring the AP III absorbance signal. This allowed simultaneous use of the two indicators with essentially no change in the elements of our previous optical system for AP III. The simultaneous recordings provided data for calibrating the fura-2 signal in muscle fibers so as to be consistent with the AP III calcium transient (Baylor et al., 1985b; Hollingworth and Baylor, 1987; Baylor and Hollingworth, 1987). Our present results confirm the occurrence of a relatively small but prolonged elevation of [Ca^{2+}] following a large [Ca^{2+}] transient. This relatively slow component is recorded by fura-2 without interference from intrinsic signals or from signals due to changes in [Mg^{2+}] and is maintained for many seconds. Abstracts of some aspects of this work have been presented previously (Klein et al., 1987; Schneider et al., 1987b).

METHODS

Fiber Preparation and Mounting

Single twitch fibers were isolated from frog ileofibularis muscles, cut at both ends, and mounted in a double vaseline gap voltage clamp chamber (Kovacs et al., 1983). Final dissection and mounting were carried out in a calcium-free, high-potassium relaxing solution (Kovacs et al., 1983). Fibers were stretched to sarcomere lengths of 3.7–4.5 μm to eliminate fiber movement, which otherwise would have produced artifacts in the optical light absorbance records. After forming the vaseline seals, the "external" solution bathing the intact fiber segment in the middle pool and the "internal" solution applied to the cut ends were changed to solutions identical to those used previously (Melzer et al., 1986b) except that the internal solution contained two calcium indicators instead of one, 50 μM fura-2 (membrane impermeable free acid form) as well as 1 mM AP III. In some experiments 5 mM Na creatine phosphate was added to the internal solution and no calcium was added. The fibers were voltage clamped as previously described (Kovacs et al., 1983) at a holding potential of – 100 mV. Experiments were carried out at 6–10°C.

Apparatus for Simultaneous Absorbance and Fluorescence Measurements

A simplified schematic diagram of the optical system used in these experiments is shown in Fig. 1. The system was designed to allow simultaneous recording of absorbance changes at relatively long wavelengths (AP III and intrinsic signal) and fluorescence signals at shorter wavelengths (fura-2). It was assembled by modifying the compound microscope used in previous experiments, with all components for recording absorbance signals maintained as in our most recent studies (Melzer et al., 1986b; Schneider et al., 1987a). For the sake of illustration, the light at each wavelength of interest is represented by a different type of line in Fig. 1 and is shown to follow a spatially separate path. In reality, all
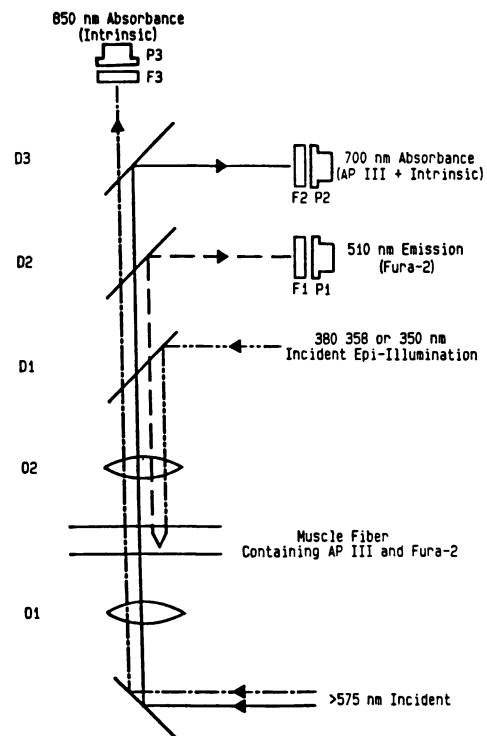

FIGURE 1 Simplified schematic diagram of the optical set-up for monitoring Ca^{2+} signals simultaneously using AP III absorbance and fura-2 fluorescence. Long wavelength light (>575 nm) from a tungsten-halogen lamp transilluminates the fiber from below, while UV light passed through a slide-selectable incident filter epi-illuminates the fiber from above. 01 and 02 are 10× air (NA 0.25) and 40× water-immersion (NA 0.75) microscope objectives, respectively. Dichroic mirrors D1, D2, and D3 reflect light of successively longer wavelengths. Filter photodiode combinations F1/P1, F2/P2, and F3/P3 record the fluorescent light intensity at 510 nm and the transmitted light intensity at 700 and 850 nm, respectively. A lens (not shown) in front of each photodiode focused the light on the active surface of the photodiode. See text for additional details.

wavelengths were spatially mixed in the apparatus. For absorbance measurements, the fiber was transilluminated with light from a tungsten-halogen lamp that was passed through an incident light cut-on filter at 575 nm (not shown) to give the bottom incident light beam in Fig. 1. The incident beam illuminated an adjustable slit (not shown), and a reduced-size image of the slit was focused on the fiber using a 10× objective (01). Transmitted light was collected with a 40× water-immersion objective (02), and the transmitted light intensities at 700 and 850 nm were monitored simultaneously using the top dichroic beam splitter (D3) and the filter-photodetector units F2/P2 (700 nm) and F3/P3 (850 nm). This much of the apparatus was identical to that used previously for recording AP III and intrinsic signals from cut fibers (Melzer et al., 1986b).

To record the fura-2 fluorescence signal together with the absorbance signals, we made several additions to the previous system. Two new dichroic beam splitters (D1 and D2 in Fig. 1) were incorporated between the water immersion objective (02) and the original dichroic beam splitter (D3). The bottom beam splitter (D1; DC 400 LP, Omega Optical Inc., Brattleboro, VT) reflected light of ~300–400 nm while transmitting light outside this band. It was used with an incident light illuminator (2090 vertical illuminator, Reichert Scientific Instruments, Buffalo, NY) equipped with 75-W xenon lamp and selectable interference filters (380, 358, and 350 nm, 10-nm bandwidth; Omega Optical Inc.; not shown) to epi-illuminate the fiber with an incident UV light beam as shown in Fig.

1. A round aperture (not shown) was positioned in the illuminator so that a reduced-size image of the aperture was produced in the object plane of the water immersion objective 02, giving a spot of UV light at this position. During an experiment the microscope was focused on the muscle fiber so that the spot of UV light was focused on the fiber. The diameter of the spot was equal to the length of the slit used for transillumination. A fraction of the fura-2 fluorescence resulting from the UV illumination of the fiber was collected by the water immersion objective. Because fura-2 fluorescence emission is centered at 510 nm (Grynkiewicz et al., 1985), the emitted light passed through beam splitter D1 but was reflected by beam splitter D2 (DC 550 LP, Omega Optical Inc.), which reflected light between ~450 and 550 nm. The light reflected by D2 was monitored by filter-photodetector unit F1/P1, which consisted of a 510 nm interference filter (40-nm bandwidth; Omega Optical Inc.) followed by a photodiode (EG & G, Salem, MA, UV-215BG) and current measuring operational amplifier with 1,000 MΩ feedback resistor, to give the fluorescence at 510 nm. The time constant of the circuit for detecting fura-2 fluorescence was found to be 0.5 ms using a light-emitting diode positioned in place of the muscle fiber.

The period of UV illumination was limited to the sampled interval using a computer-controlled shutter (Ealing Corp., S. Natick, MA; 22-8411 with custom interface) incorporated into the xenon lamp housing. Fluorescence measurements were taken as the difference in the output of the 510 nm recording system with the shutter open and closed. Periodic UV illumination minimized the bleaching of fura-2 over the course of the experiment. During single records bleaching of fura-2 caused negligible change in fluorescence, even at the slowest sampling rates, as verified by fluorescence recordings in the absence of fiber stimulation.

The transmitted light originating from the tungsten-halogen source (bottom of Fig. 1) and monitored for the absorbance signals (top) was at 700 and 850 nm and thus passed through both D1 and D2 with little attenuation. For this reason, the addition of the optical elements needed for fluorescence measurements made little change in the performance of the previous system for recording absorbance signals. There was essentially no "cross-talk" between the fluorescence and absorbance signals. The incident beam from the tungsten-halogen source (bottom) contained wavelengths almost entirely beyond the transmission band of the 510-nm filter and thus made little contribution to the output of the 510-nm fluorescence recording system. In addition, any output of the 510-nm system due to light from the tungsten-halogen source was canceled while taking the difference in 510-nm outputs with the UV source shutter open and closed because the halogen source was not interrupted by the shutter. The absorbance signals were not influenced by fura-2 fluorescence because they were monitored at 700 and 850 nm, which are well beyond the emission band of fura-2.

Fura-2 Fluorescence Measurements

The background fluorescence was recorded for each excitation wavelength in each experiment before dye entry and was subtracted from all subsequent fluorescence measurements. In several cases the background fluorescence was redetermined at the end of the experiment by removing the fiber from the chamber and was found to be essentially the same as at the start of the experiment. Fura-2 signals were calculated as the ratio (R) of fura-2 fluorescence at 380 nm excitation (F_{380}) to that at 358 nm excitation (F_{358}). The resulting signals are presented as $-R$ so that an increase in [Ca^{2+}] corresponds to a rise in the ratio signal $-R$. Fluorescence excitation at 358 nm was achieved by slightly tilting a 360-nm filter until no change in fluorescence was observed for pulses that gave large signals at 380 nm. Use of a 355-nm filter gave signals of opposite polarity to the untilted 360-nm filter. Thus our tilted filter, which we refer to as nominally 358 nm, was between 355 and 360 nm. The use of fluorescence ratios corrects the fura-2 signals for the effects of varying pathlengths and concentrations of fura-2 (Grynkiewicz et al., 1985) and thus provides a signal that can be readily converted to [Ca^{2+}]. Because the fura-2

fluorescence for 358 nm excitation is insensitive to [Ca^{2+}] (Grynkiewicz et al., 1985 and Fig. 4), the value of F_{358} in the resting fiber was used to normalize each F_{380} record. F_{358} was monitored at intervals of ~10–20 min during the course of the experiment, and its value at the time of each F_{380} signal was determined by temporal interpolation.

Determination of [Ca^{2+}] from the Fura-2 Fluorescence

The equilibrium relationship between [Ca^{2+}] and the fraction (CaD) of fura-2 reacted with calcium is

$$[Ca^{2+}] = K_D \, CaD/(1 - CaD), \qquad (1)$$

where K_D is the dissociation constant of the calcium fura-2 reaction. The observed fura-2 ratio signal $-R$ ($= -F_{380}/F_{358}$) is a linear function of the percent saturation of fura-2 by calcium, ranging from $-R_{min}$ at 0% Ca-fura-2 to $-R_{max}$ at 100% Ca-fura-2. CaD is thus given by

$$CaD = (R - R_{min})/(R_{max} - R_{min}). \qquad (2)$$

Substituting Eq. 2 into Eq. 1 gives

$$[Ca^{2+}] = K_D \, (R - R_{min})/(R_{max} - R). \qquad (3)$$

Eq. 3 can be obtained directly from Eq. 5 of Grynkiewicz et al. (1985) for the condition that the reference wavelength be the isosbestic wavelength. Eq. 3 allows calculation of [Ca^{2+}] from our fura-2 ratio signals from muscle fibers under the assumption of instantaneous equilibration of calcium with fura-2 or for the condition that [Ca^{2+}] is changing sufficiently slowly that the Ca-fura-2 reaction is always at equilibrium.

When [Ca^{2+}] was changing sufficiently rapidly that fura-2 was not at equilibrium, which appeared to be the case for most [Ca^{2+}] transients produced by pulse depolarizations, CaD could be calculated from the differential equation

$$dCaD/dt = k_{on} [Ca^{2+}] (1 - CaD) - k_{off} CaD, \qquad (4)$$

where k_{on} and k_{off} are the forward and reverse rate constants for the Ca-fura-2 reaction. In this case [Ca^{2+}] was calculated from the fura-2 ratio signal using

$$[Ca^{2+}] = \frac{dR/dt + k_{off} (R - R_{min})}{k_{on} (R_{max} - R)}, \qquad (5)$$

which is obtained by substituting Eq. 2 into Eq. 4. The values of the fura-2 reaction rate constants used in Eq. 5 as well as the value of $-R_{max}$ were determined in each fiber as described in the results section. The derivative in Eq. 5 was calculated using a seven-point least-squares cubic convolution method (Ratzlaff, 1987, p. 393) to minimize the noise introduced into the [Ca^{2+}] record.

Calibration of Fura-2 Fluorescence and Measurement of Dye Concentrations

Our system for fura-2 fluorescence measurements was tested using several thin-walled glass capillary tubes of different diameters, each filled with a calibrating solution containing fura-2 and positioned in our chamber in place of a muscle fiber. The tube internal diameters were chosen to bracket the range of muscle fiber diameters in our experiments. All other aspects of the apparatus were identical to those used during an actual experiment. The fluorescence at 510 nm was determined with various calibrating solutions in the tube using 380, 358, or 350 nm excitation. Other independent tests on our set-up showed that a layer of glass thicker than the wall thickness of the tube did not absorb a significant amount of light at 380, 358, or 350 nm. However, we cannot rule out the possibility that some of the spectral differences we observed

between fura-2 in the tube and in a muscle fiber might arise from differences in the wavelength dependence of the refractive or scattering properties of a glass tube and a muscle fiber. The spectral characteristics of calibrating solutions were occasionally checked in a commercial spectrofluorometer (Aminco-Bowman, Silver Spring, MD).

To determine the actual concentration of fura-2 in a muscle fiber, we required an absolute calibration of our apparatus. This was obtained by using capillary tubes of three different internal diameters ($d = 65, 75$, and 110 μm) in place of the fiber. Each tube was filled successively with internal solution containing fura-2 at each of four different concentrations (10, 25, 50, or 75 μM) and the fluorescence was measured in each case using 358 nm excitation. AP III was not present in these calibrating solutions. The measured F_{358} was plotted as a function of d^2 for each concentration of fura-2. For each of the four concentrations a linear relationship was obtained. The resulting four lines were consistent with the same calibration relationship,

$$[\text{fura-2}] = I \, F_{358}/d^2, \tag{6}$$

in which I is a calibration factor and F_{358} is the measured fluorescence intensity for 358 nm excitation. A single value of I was consistent with the results for all tube diameters and concentrations. The value of I is specific to our apparatus, depending on the geometrical arrangement of optical elements and their optical properties, and on the light intensity of the xenon source. The latter was checked periodically between experiments.

AP III absorbs appreciably at both the excitation (358 nm) and emission (510 nm) wavelengths of fura-2. It was thus necessary to correct the measured fluorescence for the effects of the AP III present in the fiber before using Eq. 6 to determine the fura-2 concentration in a fiber. To correct for this "inner filter" effect due to AP III, the measured fluorescence at 358 nm excitation was scaled by a factor, f, given by

$$f = \frac{1 - 10^{-(a \, A_{550})}}{\ln 10 \, a \, A_{550}}, \tag{7}$$

where A_{550} was the measured absorbance of the fiber at 550 nm due to AP III. A derivation of Eq. 7 is presented in the Appendix. The value of the coefficient a used in Eq. 7 was determined from fluorescence measurements of internal solution containing 50 μM fura-2 and several different concentrations of AP III in a glass capillary tube positioned in place of the fiber. The cytosolic concentration of fura-2 was calculated from the corrected fluorescence using Eq. 6 but assuming only 70% of the fiber volume to be accessible to the dye (Baylor et al., 1983) and setting d equal to the geometric mean of the fiber diameters measured in the directions parallel and perpendicular to the microscope axis (Kovacs et al., 1983). It should be noted that present estimates of fura-2 concentration in muscle fibers are based on the assumption that for 358 nm excitation and 510 nm emission the absolute absorbance and fluorescence efficiency of fura-2 were the same in muscle fibers and in solutions in a glass tube on our setup. There was no way to verify this assumption directly because no independent measure of fura-2 concentration in a fiber was available.

The cytosolic concentration of AP III was determined from absorbance measurements on the resting fiber at 550 and 790 nm as previously described (Kovacs et al., 1983), again assuming 70% aqueous volume. For absorbance measurements on resting fibers D2, D3, and F3 (Fig. 1) were removed from the light path. One of several narrow band filters (not shown in Fig. 1) was then placed in the incident beam to set the incident wavelength, and P3 was used to record the light intensity with and without the fiber in the light path. The measurements of AP III and fura-2 concentrations were carried out at various times during the course of an experiment. The dye concentration at the time of each pulse was determined by linear temporal interpolation between measurements.

Data Recording and Analysis

The relatively small changes in fiber absorbance accompanying pulse depolarizations were recorded in our earlier experiments using the previously described track-and-hold circuit (Kovacs et al., 1983). More recently we used the dual-mode photodiode circuit of Irving et al. (1987), operating in the sample-and-hold mode. Absorbance signals recorded at 700 nm were corrected for dye-independent intrinsic components by subtracting the simultaneously recorded 850-nm absorbance signal scaled by $(850/700)^{1.2}$ before calculating the calcium transient (Melzer et al., 1986b). The fura-2 fluorescence signal was recorded directly without use of a track-and-hold system.

Calcium transients were calculated from the AP III absorbance signals using the calibration of Kovacs et al. (1983). Although the values of dissociation constant and extinction coefficient change obtained in that calibration have recently been questioned (Hollingworth et al., 1987), the calibration of Kovacs et al. still provides a valid empirical relationship between the measured absorbance change and the change in $[Ca^{2+}]$ for a given concentration of AP III. However, if an appreciable fraction of the AP III in the fiber were bound to myoplasmic constituents (Maylie et al., 1987, and present data) and if bound AP III were unreactive with calcium, the actual calcium transients would be larger than calculated here (Maylie et al., 1987). Various alternative possibilities regarding the AP III calibration in muscle fibers are considered in the results section in relation to the present simultaneous recordings with AP III and fura-2.

All optical signals as well as membrane current and voltage were monitored using an A-to-D converter (Data Translation DT 2801A) in a personal computer (Zenith Z158) and stored on hard or floppy disk for subsequent analyses. The three optical and two electrical signals were successively sampled at 40-μs intervals to give one value for each signal. This sampling sequence was repeated at regular intervals to give the records presented here. Pulse sequences and timing of data acquisition were set by a computer-programmable pulse generator system (University of Rochester Department of Physiology Electronics Shop) which allowed variation of sampling rates within a record. In general, fura-2 signals were sampled with the shutter continuously open during the record. However, in a few experiments a "slow sampling" mode was used for monitoring the fura-2 fluorescence signal at 5-s intervals. In this case the output voltage of the fluorescence monitoring amplifier was first sampled 50 times with the shutter of the UV light source closed. The shutter was then opened for 1 s during which 250 equally spaced determinations of the fluorescence output were obtained. The shutter was then closed for 4 s until the next point was sampled. Each point in the fluorescence record was calculated as the difference of the average values with the shutter open and closed.

Nonlinear least-squares curve fitting was carried out using the procedure of Scarborough (1966), with estimates of errors of individual parameters calculated as described by Cleland (1967). Curve fitting programs were written in FORTRAN 77 and compiled and executed on a 32-bit processor board (Definicon Systems, Westlake Village, CA, DSI-32) with its own on-board memory running in a Zenith Z158 computer.

RESULTS

Time Course of Dye Entry

Fig. 2 presents data concerning the time course of dye entry into muscle fibers in our setup. The solid circles and right ordinate scale in Fig. 2 A present the concentration of AP III in the central region of a fiber, plotted as a function of time after the solution containing both AP III and fura-2 was first applied to the two cut ends of the fiber. After an initial delay of ~20 min the AP III concentration in the central region of the fiber increased continuously and approximately linearly during the subsequent 3-h duration of the experiment, with no indication of a decreasing rate of entry.
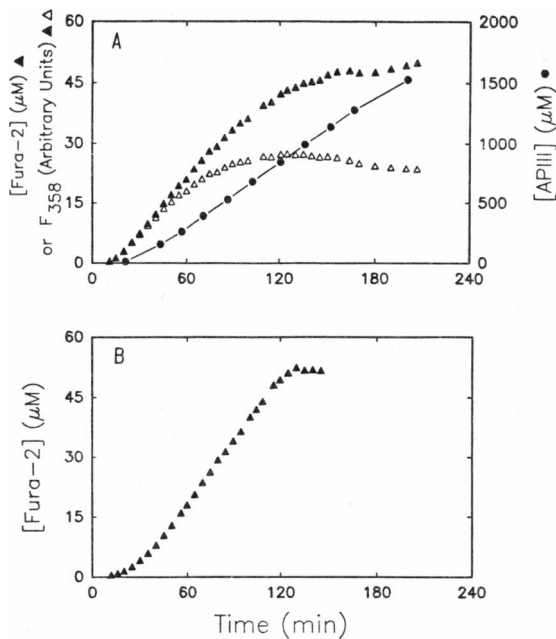
The fura-2 fluorescence due to illumination of the

FIGURE 2 Time course of entry of AP III and fura-2 into muscle fibers. At time = 0, internal solution containing 50 μM fura-2 and 1 mM AP III (A) or 50 μM fura-2 and no AP III (B) was applied to the end-pools. Subsequently, the concentration of AP III and the emitted fluorescence at 358 nm excitation due to fura-2 (F_{358}) were measured in the central recording pool at various times. (A) *Solid circles and right ordinate*, concentration of AP III in the fiber in the central pool, calculated as described in the text. *Open triangles*, F_{358} measured from the fiber in the central pool (arbitrary scale). *Solid triangles*, F_{358} after correction for the absorption of incident and emitted light by AP III as described in the text. The solid triangles (and left ordinate scale) also give the concentration of fura-2 in the fiber calculated from the corrected F_{358}. Fiber VI217, 10°C, diameter 105 μm, 3.9 μm per sarcomere. (B) Concentration of fura-2 in another fiber exposed to fura-2 but no AP III in the end pools. In this case no correction was needed for AP III absorbance and the fura-2 concentration was calculated directly from the measured F_{358} by Eq. 6. Fiber VI237, 10°C, diameter 80 μm, 4.0 μm per sarcomere. The fiber membrane potential was held at 0 mV throughout the course of both experiments.

central region of the same fiber with 358 nm light is given by the open triangles in Fig. 2 A. The fura-2 fluorescence began to increase after a shorter delay than observed for the rise of AP III, reached a maximum value by ~2 h after dye application and then began to decline slowly with time. However, the measured fura-2 fluorescence did not provide a linear measure of the fura-2 concentration because the AP III concentration and consequent suppression of fura-2 fluorescence due to light absorbance by AP III (Methods) was increasing with time. The measured fura-2 fluorescence was therefore corrected for the effects of AP III absorbance (Eq. 7) to give the solid triangles in Fig. 2 A. Comparison of the corrected and uncorrected fluorescence measurements (solid and open triangles in Fig. 2 A) indicates that by the end of this experiment AP III absorbance suppressed as much as half of the fura-2 fluorescence. The corrected fluorescence was converted,

according to Eq. 6 with our calibration factor and the measured fiber diameter, to give the actual fura-2 concentration in the central region of the fiber (solid triangles relative to the left ordinate scale in Fig. 2 A). The fura-2 concentration increased continuously during the first 2.5 h of the experiment, but by ~2.5–3 h after dye application approached a steady level which was approximately equal to the 50 μM concentration of fura-2 in the solution applied to the cut ends of the fiber.

The results in Fig. 2 A indicate that fura-2 entered the fiber more rapidly than AP III. The fura-2 concentration in the center of the fiber reached equilibrium with the end pool solution while the AP III concentration was still increasing at a relatively rapid rate. Because the concentrations of AP III or fura-2 in Fig. 2 A were calculated, respectively, from total fiber absorbance or fluorescence due to dye, they do not distinguish between free dye and dye bound to myoplasmic constituents. However, the fact that the calculated equilibrium concentration of fura-2 in the fiber was equal to the end pool concentration suggests that little fura-2 was bound within the fiber. In contrast, the calculated concentration of AP III at the end of the experiment was 50% greater than the concentration in the end pool and was still increasing at a relatively rapid rate. This confirms the recent observations and interpretation of Maylie et al. (1987) that an appreciable fraction of the AP III in a fiber may be bound to myoplasmic constituents.

The conclusion from Fig. 2 A that the equilibrium concentration of fura-2 was approximately equal to the end pool concentration depended heavily on the correction for AP III light absorbance. To avoid this correction, we monitored the dye entry time course in another fiber in which fura-2 but no AP III was added to the end pool solution. The time course of fura-2 entry into that fiber is presented in Fig. 2 B and is quite similar to the corrected time course (solid triangles in Fig. 2 A) measured in the presence of AP III. The concentration of fura-2 in this fiber at the end of the experiment also reached a steady level about equal to the concentration in the end pools, confirming the results in Fig. 2 A.

Spectral Properties of Fura-2 in Resting Muscle Fibers

The mean value of $-R(= -F_{380}/F_{358})$ in 18 resting fibers was -1.35 ± 0.05 ($\pm$SEM) about 1 h after exposing the cut ends of the fibers to internal solution containing 50 μM fura-2 and 1 mM AP III. In contrast, the value of $-R$ obtained using internal solution with 10 μM or 50 μM fura-2 in a glass capillary tube on our set-up was -1.10, with or without AP III. The value of $-R$ should increase linearly with the fraction of fura-2 complexed by calcium, which in turn increases with increasing $[Ca^{2+}]$. Thus the difference in $-R$ in resting fibers and in internal solution in the calibrating tube could indicate that the level of $[Ca^{2+}]$ was lower in fibers than in internal solution.

However, measurements with stronger calcium buffering indicated that there was actually a difference in the spectral properties of calcium-free fura-2 in fibers and in solution.

Using internal solution to which 1 mM EGTA was added (no added calcium), the mean value of $-R$ for fura-2 in three fibers was -1.91 (± 0.15 SEM), whereas the value of $-R$ in the same solution in the calibrating tube was -1.37 with or without AP III. Increasing the concentration of EGTA to 5 or 70 mM caused no change in the value of $-R$ for the solution in the tube, indicating that the tube value corresponded to calcium-free fura-2 in solution. The value of $-R$ found in fibers exposed to internal solution plus 1 mM EGTA was more negative than -1.37 and would thus indicate a negative value of $[Ca^{2+}]$ in muscle fibers if the tube calibration were to be applied to fura-2 in muscle fibers. It therefore appears that the spectral properties of calcium-free fura-2 in fibers must differ from those determined for calcium-free fura-2 in solution in a tube on our set-up. Similar observations and conclusions regarding the properties of fura-2 in cells and in solution were obtained by Almers and Neher (1985) in mast cells exposed to an internal solution containing fura-2 and EGTA from a patch pipette. For conversion of fura-2 signals in muscle fibers to $[Ca^{2+}]$ records we therefore used the value of $-R_{min}$ determined in fibers exposed to internal solution plus 1mM EGTA. If 1 mM EGTA were insufficient to remove all calcium from fura-2 in the fibers, the calcium levels calculated using this value would be systematically underestimated.

To experimentally test whether $[Ca^{2+}]$ in muscle fibers could be set lower than the level attained with 1 mM EGTA, we exposed six fibers to internal solution containing 70 mM Cs_2EGTA (by substitution for 103 mM Cs glutamate). Surprisingly, the value of $-R$ in this case was -1.54, indicative of a higher rather than a lower level of $[Ca^{2+}]$ in these fibers compared with those exposed to

internal solution containing 1 mM EGTA, where $-R$ was -1.91. The source of this unexpected effect of high EGTA concentration was not further investigated.

Comparison of AP III and Fura-2 Signals

When depolarizing pulses were applied to fibers containing both fura-2 and AP III, the fura-2 fluorescence ratio signal (Fig. 3 A) and the AP III absorbance change (Fig. 3 B) were both consistent with a transient rise of $[Ca^{2+}]$. However, the families of signals generated by the two indicators showed considerable differences, even though they were recorded simultaneously in response to the same calcium transients. Three points are noteworthy concerning the families of records generated by the two indicators. First, as the fiber membrane potential during the pulse was increased from -50 to -20 mV in 10-mV steps, the AP III signal increased appreciably and by roughly similar amounts with each 10-mV increment (Fig. 3 B). In contrast, the fura-2 signal (Fig. 3 A) increased appreciably as the pulse increased from -50 to -40 mV, but then increased only slightly for the pulses to -30 and -20 mV. The observation that the fura-2 fluorescence approached saturation for a range of calcium transients which did not saturate the AP III response was made in all fibers studied and is consistent with the higher calcium affinity of fura-2 (Grynkiewicz et al., 1985) compared to AP III (Rios and Schneider, 1981; Kovacs et al., 1983; Hollingworth et al., 1987) in calibrating solutions.

Second, after the pulses in Fig. 3, the AP III absorbance signals (Fig. 3 B) for the three smaller pulses declined to close to their starting levels and only the AP III signal for the largest pulse exhibited a slight remaining elevation at the end of the record. In contrast, the fura-2 fluorescence signals (Fig. 3 A) were all still appreciably elevated at the end of each record, with the amount of elevation increasing with the amplitude of the preceding depolarizing pulse.
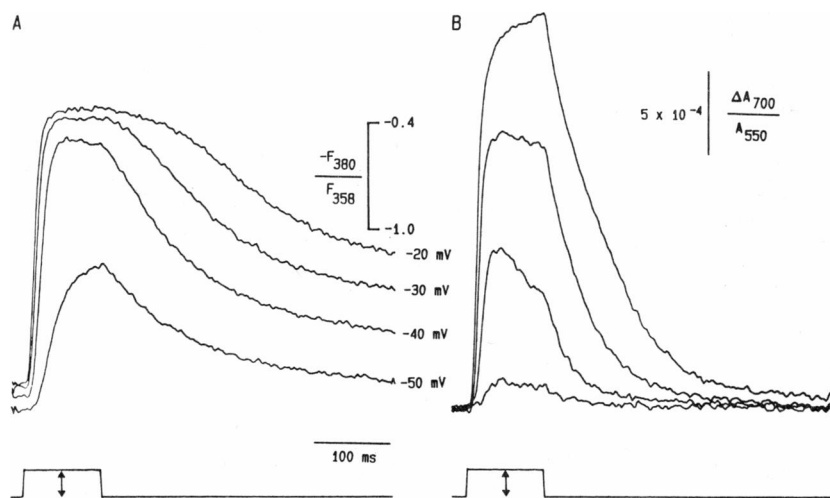

FIGURE 3 Comparison of simultaneously recorded fura-2 and AP III signals for depolarizing pulses of various amplitudes in a voltage-clamped skeletal muscle fiber. (A) Ratio signals (R) of fura-2 fluorescence at 380 nm excitation (F_{380}) to that at 358 nm excitation (F_{358}) for 100-ms pulses from -100 mV to the indicated membrane potential. Each signal is presented as $-R$. The changes in baseline levels of the signals indicate that the resting $[Ca^{2+}]$ increased during the course of the recordings, from 13 to 27 nM using the calibration values in Fig. 6, legend. (B) Antipyrylazo III absorbance signals ΔA_{700} at 700 nm recorded simultaneously with the fura-2 signals in A and corrected for changes in AP III concentration by dividing by the resting absorbance A_{550} due to AP III at 550 nm. The total absorbance signal at 700 nm was corrected for dye-independent intrinsic components by subtracting the simultaneously recorded 850 nm absorbance signal scaled by $(850/700)^{1.2}$ (Melzer et al., 1986b). Each record in A and B is the average of four successive applications of the same pulse at 30- or 45-s intervals. The AP III concentration increased from 393 to 460 μM for the sequence in A and B while F_{358} increased by 8%. Fiber 377, 3.9 μm per sarcomere, 9.0°C.

The elevated fura-2 signal at the end of each record, with little or no elevation of the corresponding AP III signal, is again consistent with the difference in calcium affinities of the two indicators.

Third, the fura-2 fluorescence signals before the pulses in Fig. 3 A had different baseline levels. This was not due to changes in fura-2 concentration, which were normalized by forming the fluorescence ratio, but indicates a true change in fiber $[Ca^{2+}]$ before the pulses. Such changes in resting calcium could be detected with fura-2, but could not be monitored effectively with the lower affinity AP III.

Excitation Wavelength Dependence of Fura-2 Signals

Before examining further the differences in the fura-2 and AP III signals we investigated the wavelength dependence of the fura-2 signals to determine whether any fluorescence components due to changes in $[Mg^{2+}]$ were present in the fura-2 signals recorded from muscle fibers. The results presented in Fig. 4 are qualitatively inconsistent with the presence of significant components due to changes in $[Mg^{2+}]$ in the fura-2 signals. The upper record in Fig. 4 A was obtained at 380 nm excitation by repeating the pulse to -30 mV in Fig. 3, but now recording on a slower time scale. The lower record is for the same pulse and time base, but with excitation at 358 nm (Methods). In calibrating solutions, raising $[Mg^{2+}]$ produces a much larger increase in fura-2 fluorescence at 358 nm excitation than at 380 nm, whereas 358 nm is an isosbestic wavelength for the Ca-fura-2 reaction (Grynkiewicz et al., 1985). The relatively large fiber fluorescence signal obtained with 380 nm excitation together with the absence of any significant signal for 358 nm excitation (Fig. 4 A) thus indicates that any magnesium component in the 380 nm signal must have been negligible if the dye had qualitatively similar properties in the fiber and in the calibrating solutions.

Fig. 4 B presents fura-2 fluorescence signals from another fiber for excitation at 380 (top) and 350 nm (bottom). In calibrating solutions formation of calcium-fura-2 causes a decrease of fluorescence for 380 nm excitation and an increase in fluorescence for 350 nm, whereas formation of Mg-fura-2 causes little fluorescence change for 380 nm and a relatively large increase in fluorescence for 350 nm (Grynkiewicz et al., 1985). Thus, the opposite polarity but similar time course of signals for 380 and 350 nm excitation in muscle fibers (Fig. 4 B) are as expected for an increase in fiber $[Ca^{2+}]$ during the pulse. The records for 380 and 350 nm excitation in Fig. 4 B were arbitrarily scaled to have the same peak value. The record in the center of Fig. 4 B is the sum of the top and bottom records. The fact that it is essentially flat demonstrates that the signals at 380 and 350 nm excitation had the identical temporal waveform. Given the difference in spectral properties of the calcium- and magnesium-fura-2 complexes, the only way that a significant magnesium component could have been present in the fura-2 signals at 380 and 350 nm in Fig. 4 B would be for the magnesium and calcium signals to have had the same temporal waveform. This is highly unlikely because the changes in myoplasmic $[Ca^{2+}]$ and $[Mg^{2+}]$ appear to follow very different time courses (Baylor et al., 1982a and b).

Comparison of Fura-2 Signals in Fibers and in Calibrating Solutions

The excitation wavelength dependence of fura-2 signals from muscle fibers (Fig. 4 and other fibers) differed quantitatively from the wavelength dependence of the fluorescence changes due to raising $[Ca^{2+}]$ in fura-2 solutions in a glass tube on the same set-up. The latter were determined from differences in fluorescence between internal solution with 1 mM added EGTA or with 0.5 mM added calcium, both containing 10 or 50 μM fura-2 and 0,
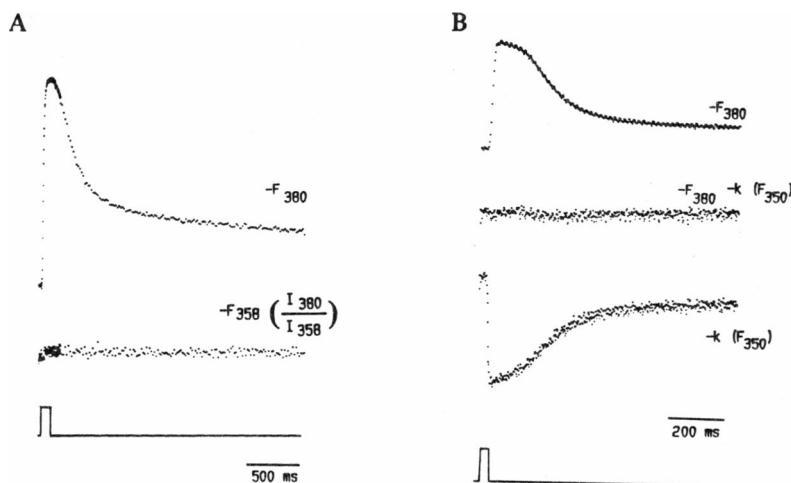

FIGURE 4 Excitation wavelength dependence of the fura-2 fluorescence signals in skeletal muscle fibers. (A) Fura-2 fluorescence signals recorded for successive applications of a 100-ms pulse to -30 mV using either 380 or 358 nm excitation and signal-averaged four times. To correct for differences in incident light intensity the signal at 358 nm was multiplied by the ratio of intensities (380/358 nm) at the level of the fiber. (B) Fura-2 fluorescence signals from another fiber for successive applications of a 30-ms pulse to -20 mV, with excitation at either 380 or 350 nm (signal-averaged three and four times, respectively). The 350-nm signal was scaled by a factor of k (-5.4) so as to have the same peak amplitude as the 380-nm signal. The middle record is the sum of the top and bottom records. The fact that it is essentially flat demonstrates that the signals at 380 and 350 nm excitation had an identical temporal waveform. (A) Same fiber and conditions as Fig. 3. (B) Fiber 391, 4.0 μm per sarcomere, 8.5°C.

500, or 1,000 μM AP III. Fluorescence differences between these two solutions should correspond to a change from completely calcium-free fura-2 to completely calcium-complexed fura-2.

For 358 nm excitation, there was a 30% increase in fluorescence on changing from zero to saturating calcium in the fura-2 solution in the tube. Because calcium complexation increases fura-2 fluorescence below the isosbestic wavelength and decreases it above the isosbestic wavelength (Fig. 4 and Grynkiewicz et al., 1985), our nominal 358-nm filter was below the isosbestic wavelength for fura-2 solution in a tube on our set-up. In contrast, 358 nm was specifically set (Methods) to be the isosbestic wavelength for fura-2 in muscle fibers on the same set-up. The ratio of the fluorescence changes at 380 nm to 350 nm for increasing [Ca^{2+}] in the solutions was 2.7. The value of the ratio of fluorescence changes at 380 to 350 obtained from the scale factor used for the muscle fiber in Fig. 4 B was 5.4 and the mean value from five fibers was 5.9. The value of $-R_{max}$, which is equal to $-R$ when all fura-2 is complexed with calcium, was -0.11 for the high [Ca^{2+}] fura-2 solution in the tube but was found to equal -0.34 in 18 muscle fibers (Table I). Finally, $-R_{min}$, the fluorescence ratio for calcium-free fura-2, was -1.34 in solution and -1.91, or perhaps even more negative, in muscle fibers. The more negative values of both $-R_{max}$ and $-R_{min}$ in

muscle fibers compared with solutions are consistent with differences in spectral properties reported for fura-2 in PtK_1 cells and in nonviscous calibrating solutions, and attributed to increased cytoplasmic microviscosity in the cells compared with the calibrating solution (Poenie et al., 1986). Also, in intact muscle fibers, measurements of steady-state fluorescence anisotropy indicated that fura-2 in myoplasm is significantly less mobile than free dye in a salt solution at the viscosity expected for myoplasm (Baylor and Hollingworth, 1987).

All of these results demonstrate real differences in the spectral properties of fura-2 in solution in capillary tubes and fura-2 in muscle fibers on the same set-up. Because of these differences we have attempted to use parameters determined for fura-2 in the muscle fibers themselves wherever possible. It is only for calculating the concentration of fura-2 in a fiber (Fig. 2) that we use the tube calibration. All other results in this paper rely on calibrations based on the values of $-R_{min}$ and $-R_{max}$ obtained from muscle fibers. We have not determined whether the observed differences in spectral properties of fura-2 in fibers and in solution in a tube on the same set-up are due to a true difference in the state of fura-2 in solution and in a fiber or whether they are just due to some optical difference between the tube and fiber and not due to a difference in the dye.

TABLE I

FURA-2 CALIBRATION PARAMETERS FROM LEAST-SQUARES FITTING ANALYSIS

Fiber	k_{on}		k_{off}		K_D	$-R_{max}$		Resting [Ca^{2+}]	
	Value	SD	Value	SD		Value	SD	60 min	90 min
	$\times 10^8 M^{-1}s^{-1}$	$\times 10^8 M^{-1}s^{-1}$	s^{-1}	s^{-1}	nM			nM	nM
370	3.67	0.113	29.2	0.97	79.6	-0.29	0.005	17	33
377	1.11	0.015	20.6	0.29	186.4	-0.38	0.004	11	35
379	1.80	0.041	9.1	0.15	50.4	-0.69	0.006	12	22
380	1.92	0.056	10.6	0.28	54.9	-0.67	0.008	7	18
385	1.95	0.057	10.8	0.30	55.3	-0.38	0.002	36	88
386	0.98	0.027	12.8	0.32	130.8	-0.32	0.004	111	147
387	1.18	0.028	9.0	0.21	76.5	-0.34	0.004	62	130
392	1.21	0.023	12.3	0.22	101.9	-0.34	0.001	80	139
394	2.18	0.028	9.2	0.14	42.3	-0.32	0.002	28	34
396	1.25	0.011	8.5	0.08	68.1	-0.20	0.002	114	139
399	1.18	0.015	6.7	0.07	56.8	-0.23	0.002	38	55
400	1.06	0.014	5.8	0.05	56.1	-0.24	0.003	44	155
401	0.90	0.010	8.4	0.08	93.9	-0.10	0.002	67	104
402	1.36	0.008	7.4	0.07	54.6	-0.16	0.001	47	240
403	1.55	0.031	20.0	0.27	129.0	-0.24	0.006	45	82
404	2.13	0.029	14.8	0.15	69.6	-0.36	0.003	43	55
409	0.51	0.007	9.8	0.11	191.0	-0.39	0.002	71	276
411	0.94	0.008	8.9	0.06	94.9	-0.35	0.002	54	71
Mean	1.49		11.9		88.7	-0.34		49	101
SEM	± 0.17		± 1.4		± 10.5	± 0.04		± 8	± 18

Entries for k_{on}, k_{off}, and $-R_{max}$ are given as the least-squares value $\pm$ SD of the fit. K_D is k_{off}/k_{on}. Resting [Ca^{2+}] was determined from the calculated K_D and the ratio $-F_{380}/F_{358}$ in each fiber at 60 and 90 min after exposing the cut ends of the fiber to internal solution containing 1 mM AP III and 50 μM fura-2. The value of $-R_{min}$ was -1.91 for each fiber, temperature 8–10°C. In fibers 399–411 the normal internal solution (Kovacs et al., 1983) was replaced by a similar solution, but without any added [Ca^{2+}] and with 5 mM Na_2 creatine phosphate.

Calcium Transients Calculated from the AP III and Fura-2 Signals

The fura-2 fluorescence signals were consistently slower than the simultaneously recorded AP III absorbance signals (Fig. 3 and other fibers). The excitation wavelength dependence of the fura-2 signals indicated that components due to slow changes in $[Mg^{2+}]$ cannot be the cause of the slow fura-2 signals. The next point to consider was whether the difference in time course could simply be a result of calcium saturation of the dyes leading to nonlinearity in the relationships between $[Ca^{2+}]$ and fura-2 fluorescence or AP III absorbance. For fura-2 the nonlinearity could be quite severe due to near maximal complexation of this relatively high affinity indicator with calcium during a relatively large calcium transient. For AP III the relationship should be closer to linearity due to lower fractional calcium complexation of this relatively lower affinity indicator during a calcium transient. To correct for the effects of indicator saturation, calcium transients were calculated from the fura-2 and AP III signals assuming both dyes to be in instantaneous equilibrium with $[Ca^{2+}]$.

Fig. 5 A presents calcium transients for a 30-ms pulse to -20 mV calculated from simultaneously recorded fura-2 and AP III signals assuming instantaneous equilibration of both dyes with calcium. Conversion from the observed fura-2 ratio signal to $[Ca^{2+}]$ under the assumption of instantaneous equilibration of calcium with fura-2 (Eq. 3) required values of two parameters, $-R_{max}$ and $-R_{min}$. The value of $-R_{max}$ (-0.40) used in Fig. 5 A was the maximum value of $-R$ observed for large pulses applied to this fiber (not shown), and $-R_{min}$ was set to -1.91. For comparison of time courses, the two calculated calcium transients have been arbitrarily scaled to the same peak amplitude. The calcium transient calculated from the AP III signal is clearly faster than the one calculated from fura-2, indicating that the two indicators cannot both be faithfully monitoring the same actual calcium transient. The time course of at least one of the calculated calcium transients must be distorted.

The $[Ca^{2+}]$ transient calculated from the fura-2 signal assuming instantaneous equilibration of fura-2 with $[Ca^{2+}]$ is a function of the parameters $-R_{max}$, $-R_{min}$, and K_D (Eq. 3). It was thus important to determine whether the fura-2 $[Ca^{2+}]$ transient could have been artifactually slowed by improper estimation of the values of those parameters. K_D appears as a simple scaling factor in Eq. 3 and thus cannot influence the time course of a fura-2 $[Ca^{2+}]$ record scaled to a set peak as in Fig. 5 A. Because the maximum observed value of $-R$ could be less than the true value of $-R_{max}$ we arbitrarily increased the value of $-R_{max}$ to -0.30, which was slightly more positive than the mean value of $-R_{max}$ obtained from 18 fibers (Table I). The recalculated and scaled fura-2 calcium transient (not shown) had essentially the same time course as the fura-2 calcium transient in Fig. 5 A. Because the value of $-R$ in 1
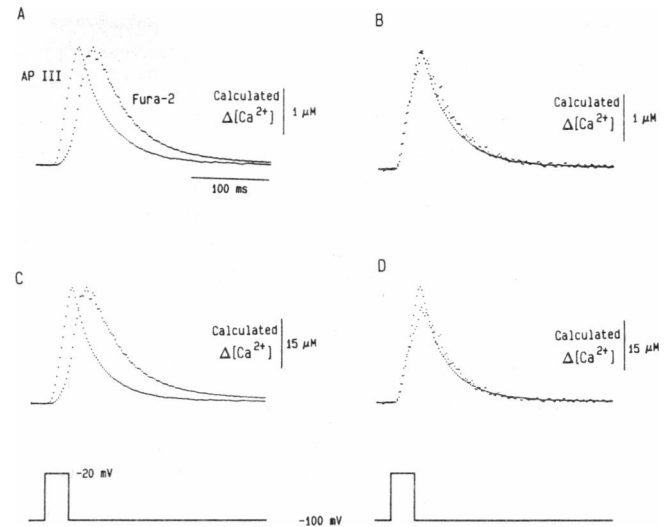

FIGURE 5   A comparison of $[Ca^{2+}]$ transients calculated from simultaneous measurements of AP III absorbance and fura-2 fluorescence using various alternative assumptions regarding the properties of the dyes in muscle fibers. These transients were elicited by a 30-ms depolarizing pulse to -20 mV. All $[Ca^{2+}]$ transients calculated from the AP III absorbance change were obtained assuming instantaneous equilibration of Ca^{2+} and AP III. (A and C) $[Ca^{2+}]$ transients calculated from AP III absorbance and fura-2 fluorescence ratio changes assuming instantaneous equilibration between fura-2 and $[Ca^{2+}]$ (Eq. 3). The fura-2 $[Ca^{2+}]$ record was scaled to match the peak of the AP III signal. In C the $[Ca^{2+}]$ transient calculated from the AP III absorbance change was obtained assuming only one-third of the total AP III in the fiber to be available to bind calcium. Note the 15-fold difference in the calibration scales (far right). (B and D) The same $[Ca^{2+}]$ transients calculated from AP III as shown in A and C are replotted together with $[Ca^{2+}]$ transients calculated from fura-2 assuming finite on and off rate constants for $[Ca^{2+}]$ binding to fura-2. The on and off rate constants were determined by least-squares fitting of the fura-2 calcium occupancy calculated from the AP III $[Ca^{2+}]$ record to the observed fura-2 ratio signal (see text). (B) $k_{on} = 0.53 \times 10^8$ $M^{-1}s^{-1}$; $k_{off} = 10.2$ s^{-1}. (D) $k_{on} = 0.04 \times 10^8$ $M^{-1}s^{-1}$; $k_{off} = 8.9$ s^{-1}. In all fura records $-R_{max} = -0.40$ and $-R_{min} = -1.91$. Fiber 409, 9.0°C, diameter 80 μm, 4.0 μm per sarcomere.

mM EGTA might not correspond to completely calcium-free fura-2, we next arbitrarily decreased the value of $-R_{min}$ to -2.2. This change also had no effect on the scaled fura-2 calcium transient (not shown). It thus appears that the time course of the calcium transient calculated from the fura-2 signal assuming instantaneous equilibration of $[Ca^{2+}]$ with fura-2 will be essentially the same over the reasonable range of values of $-R_{min}$ and $-R_{max}$.

Each of our measured signals gives the spatial average of fluorescence or absorbance over the entire illuminated region of the fiber. Theoretical calculations have shown that for certain parameter values rather steep spatial gradients of $[Ca^{2+}]$ may be predicted to exist within a single half sarcomere, especially during the relatively rapid phase of calcium release (Cannell and Allen, 1984). This raises the question of whether the difference in time course of the fura-2 and AP III signals could be due to spatial

nonuniformity of $[Ca^{2+}]$ in a fiber. Model calculations (not shown) using simplifying assumptions indicated that if both fura-2 and AP III are assumed to equilibrate instantaneously with $[Ca^{2+}]$, spatial gradients of $[Ca^{2+}]$ will not give rise to an artifactually faster calculated $[Ca^{2+}]$ signal from AP III than from fura-2. The first of two models considered two volumes with a 10-fold difference in $[Ca^{2+}]$, whereas the second model assumed a linear spatial gradient of $[Ca^{2+}]$ in one dimension. When scaled to the same peak value the $[Ca^{2+}]$ calculated from the simulated fura-2 signal rose more quickly and decayed more slowly than that calculated from the simulated AP III signal for both models. Thus, spatial gradients of $[Ca^{2+}]$ do not appear to be the source of the difference in time course of the $[Ca^{2+}]$ transients determined from fura-2 and AP III assuming both dyes to be in instantaneous equilibrium with $[Ca^{2+}]$ (Fig. 5 A).

Another interpretation of the difference in time course of calcium transients derived from the fura-2 and AP III signals in Fig. 5 A is that fura-2 equilibrates more slowly with $[Ca^{2+}]$ than does AP III. In Fig. 5 B we compare the same AP III calcium transient as in Fig. 5 A with a fura-2 calcium transient calculated assuming noninstantaneous equilibration of fura-2 with $[Ca^{2+}]$. Spatial gradients of $[Ca^{2+}]$ have been ignored here and in all further calculations in this paper. The values of $-R_{max}$ and $-R_{min}$ used to calculate the fura-2 $[Ca^{2+}]$ transient were the same as used in Fig. 5 A. The values of the on and off rate constants

$(0.53 \times 10^8 \ M^{-1}s^{-1}$ and $10.2 \ s^{-1}$, respectively) for the Ca-fura-2 reaction were chosen by a least-squares fit of the AP III signal to the fura-2 signal for this pulse using the procedure described in detail below in relation to Fig. 6. The close agreement of the two calcium transients in Fig. 5 B shows that the simultaneously recorded AP III and fura-2 signals are compatible with both indicators monitoring the same $[Ca^{2+}]$, AP III by essentially instantaneous equilibration with $[Ca^{2+}]$ and fura-2 with a kinetic delay.

Possible Influence of Bound AP III

Conversion of the AP III absorbance signal to $[Ca^{2+}]$, and in turn, the determination of fura-2 on and off rate constants depends on the AP III concentration in the fiber available to bind calcium. Careful analysis of AP III diffusion into and out of cut muscle fibers has indicated that on average about two-thirds of the AP III in a fiber may be bound to intracellular constituents (Maylie et al., 1987). A similar conclusion was reached regarding AP III injected into intact fibers (Baylor et al., 1986). This raises the possibility that the difference in time course of the $[Ca^{2+}]$ transients calculated from the AP III and fura-2 signals assuming instantaneous equilibration of both dyes (Fig. 5 A) might somehow result from the presence of bound AP III. In this case some property of bound AP III would have to make the AP III absorbance signal faster than the real $[Ca^{2+}]$ transient, rather than a kinetic delay
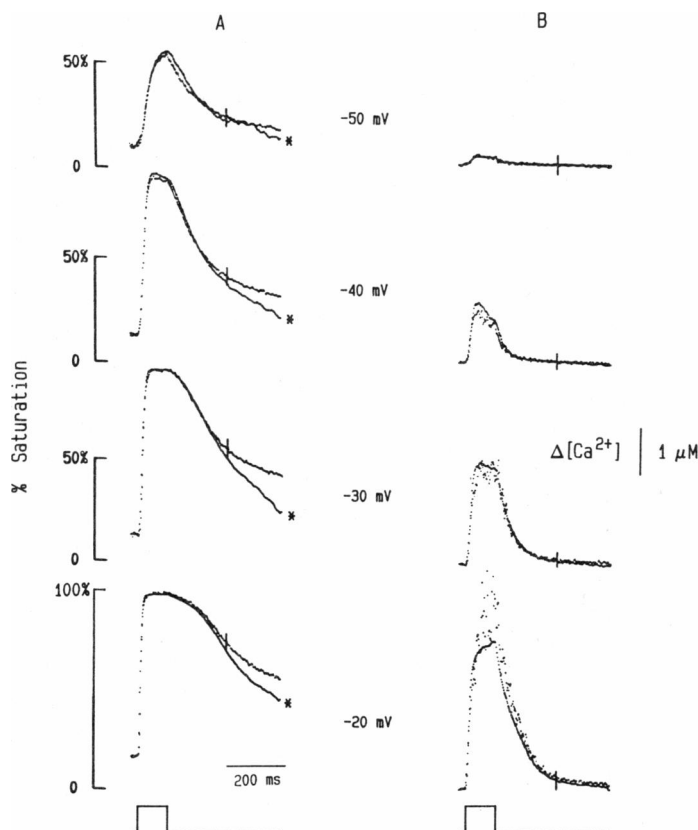

FIGURE 6 Determination of the kinetic and optical constants for the Ca-fura-2 reaction in skeletal muscle fibers so as to produce self-consistent $[Ca^{2+}]$ transients from simultaneous fura-2 and AP III signals. (A) Fura-2 signals recorded experimentally (unmarked), and superimposed theoretical fura-2 signals (*) calculated from the simultaneously recorded AP III calcium transient and fit to the experimental records. The parameter values obtained from the fit were $-R_{max} = -0.39$, $k_{on} = 1.10 \times 10^8 \ M^{-1}s^{-1}$, and $k_{off} = 17.5 \ s^{-1}$. The value of $-R_{min}$ was set to -2.00. (B) $[Ca^{2+}]$ transients calculated from AP III absorbance signals (less noisy) and from the simultaneously recorded fura-2 fluorescence ratio signals (noisier) using the same values of $-R_{min}$, $-R_{max}$, k_{on}, and k_{off} as in A. Same experimental records as in Fig. 3, A and B. The membrane potential during each pulse is indicated between the fura-2 and the $[Ca^{2+}]$ records for the pulse.

in the calcium-fura-2 reaction making the fura-2 signal slower than [Ca^{2+}] as assumed for Fig. 5 B.

Assuming that bound AP III is completely unreactive with calcium, two extreme possibilities can be considered. In the first case bound AP III is assumed to be in rapid equilibrium with free AP III. In this case all AP III in the fiber is potentially available to react with calcium during a calcium transient, but the effective dissociation constant of the calcium AP III reaction will be increased. Because the predominant Ca:AP III stoichiometry for the [Ca^{2+}] and [AP III] concentrations in muscle fibers is 1:2 (Rios and Schneider, 1981; Hollingworth et al., 1987), the value of the effective K_D will be increased by $(1/\phi)^2$, where ϕ is the fraction of calcium-free AP III that is not bound to cytoplasmic constituents. The [Ca^{2+}] transient calculated from the AP III signal using this K_D will be $(1/\phi)^2$ times larger than that in Fig. 5 A, but when scaled to the same peak value would have the identical time course. Thus, this case would not alter the relative time courses of the [Ca^{2+}] transients calculated assuming both AP III and fura-2 to be instantaneously equilibrating with [Ca^{2+}].

In the second case the AP III bound to cytoplasmic constituents is assumed to remain bound throughout the calcium transient. In this case the effective concentration of AP III will be reduced to ϕ times the total concentration of AP III in the fiber but the K_D of the unbound AP III will not be altered. The faster of the two [Ca^{2+}] records in Fig. 5 C was obtained for this case assuming two-thirds of the AP III in the fiber to be irreversibly bound and unreactive with calcium, and the remaining one-third to be in instantaneous equilibrium with [Ca^{2+}]. Its time course is actually slightly faster than the [Ca^{2+}] record calculated assuming all AP III to be available for reaction (Fig. 5 A). The change in time course of the AP III calcium transient in Fig. 5 C compared with that in Fig. 5 A arises from the greater correction for saturation of AP III by calcium when the AP III concentration is assumed to be less than the total AP III content of the fiber. The slower [Ca^{2+}] record in Fig. 5 C was obtained assuming fura-2 to be in instantaneous equilibrium with [Ca^{2+}] and is the same as the fura-2 [Ca^{2+}] record in Fig. 5 A.

In Fig. 5 D the one and off rate constants for the calcium fura-2 reaction have been adjusted to make the fura-2 [Ca^{2+}] record fit the AP III [Ca^{2+}] transient in Fig. 5 C, which is replotted in Fig. 5 D. In this case the agreement of the [Ca^{2+}] transients calculated from the two signals is not as close as in Fig. 5 B. This difference in goodness of fits could be taken as evidence that the assumption of rapid equilibration of free and bound AP III may be more reasonable than that of slow equilibration or irreversible binding.

The general conclusion from this consideration of bound AP III is that for two of the most straightforward cases to analyze the presence of bound AP III would not speed up the measured AP III signal relative the true [Ca^{2+}] transient. Thus, the presence of bound AP III cannot be

taken as an explanation for the difference of fura-2 and AP III [Ca^{2+}] transients. In general, it is easy to imagine that slow dissociation of bound AP III and its subsequent reaction with calcium could in principle give rise to a component of the AP III signal that is delayed relative to the actual [Ca^{2+}] transient, but it is difficult to imagine a reaction scheme whereby the AP III signal would be faster than the true [Ca^{2+}] transient.

Calibration of Fura-2 in Muscle Fibers

The fura-2 and AP III signals recorded simultaneously provide sufficient information to evaluate the kinetic rate constants (Baylor et al., 1985b) of the calcium-fura-2 reaction and also to calibrate the fura-2 signals to be consistent with the AP III calcium transients. The approach is based on the assumptions that both signals were produced by the same calcium transient and that noninstantaneous equilibration of the Ca-fura-2 reaction delayed the fura-2 signal relative to the true free calcium transient, which was more closely approximated by the more rapidly equilibrating AP III. The procedure is illustrated in Fig. 6. The unmarked records in Fig. 6 A are the experimentally measured fura-2 signals from Fig. 3 A, but with the ordinate scale now expressed in terms of the percent saturation of fura-2 by calcium (Eq. 2). Conversion from fluorescence ratio to percent saturation was carried out after the value of $-R_{max}$ had been determined. The starred (∗) records in Fig. 6 A are theoretical fura-2 signals calculated from the simultaneously measured AP III calcium transients (Fig. 3 B) and fit to the family of experimentally measured fura-2 signals over the interval from the start of the depolarization to the vertical line in each panel.

The fit shown in Fig. 6 was carried out using an iterative computer routine that was generally similar to the computer fitting routine used by Melzer et al. (1986a) to obtain an overall simultaneous least-squares fit of a model to several different calcium transients from the same fiber. The present program adjusted the values of the on and off rate constants (k_{on}, k_{off}) for the calcium-fura-2 reaction and the value ($-R_{max}$) of $-R$ for complete reaction of fura-2 with calcium. For Fig. 6, the values were adjusted to produce a simultaneous least-squares fit of all four theoretical fura-2 records to the experimental ones over the indicated interval. The theoretical fura-2 signals were calculated assuming AP III to be in instantaneous equilibrium with [Ca^{2+}]. The fraction of the total fura-2 in the fiber that was calcium-reacted (CaD) was obtained from the AP III [Ca^{2+}] record by numerical solution of Eq. 4 and the theoretical fura-2 ratio signal ($-R$) was calculated from CaD using a rearrangement of Eq. 2. The initial value of CaD at the start of each record was calculated from the starting value of $-R$ for that record using the values of k_{on}, k_{off}, and R_{max} from the previous iteration. The value of $-R_{min}$ could not be uniquely determined by the

fitting program, presumably because no records in Fig. 6 approached the fluorescence level for complete dissociation of calcium from fura-2. The value of $-R_{min}$ used for the fit in Fig. 6 A was within the range of values of $-R$ obtained from three other unstimulated fibers in which 1 mM EGTA was added to the cut-end solution.

The fits in Fig. 6 A were obtained using a single set of parameter values and were quite good over the entire fit interval for all records. This provides a quantitative indication that saturation and kinetic delays in the Ca-fura-2 reaction were sufficient to account for most of the differences between the AP III and fura-2 signals in Fig. 3. The parameter values obtained from the fit were $-R_{max} = -0.39$, $k_{on} = 1.10 \times 10^8$ M^{-1}s^{-1}, and $k_{off} = 17.5$ s^{-1}.

The results of fits similar to that in Fig. 6 A carried out on 18 different fibers are presented in Table I. For these fits $-R_{min}$, the limiting value of the fluorescence ratio $-R$ when fura-2 is in the calcium-free form, was set to -1.91. The mean $\pm$ SEM values of k_{on} and k_{off} were $1.49 \pm 0.17 \times 10^8$ M^{-1}s^{-1} and 11.9 ± 1.4 s^{-1}, respectively. Our mean value for k_{off} is roughly similar to the value of 25 s^{-1} (at 16°C) reported recently for fura-2 in intact frog skeletal muscle fibers by Hollingworth and Baylor (1987) and Baylor and Hollingworth (1987), using a similar method. It is much lower than the value of k_{off} of 80 s^{-1} determined in a 100 mM KCl solution at 20°C using a stopped-flow spectrofluorometer (Jackson et al., 1987). The mean value of the dissociation constant (K_D) for the Ca-fura-2 reaction, which equals k_{off}/k_{on}, was 88.7 ± 10.5 nM. This is close to the K_D value of 135 nM reported for fura-2 in calibrating solutions (100 mM KCl, 20°C; Grynkiewicz et al., 1985). If an appreciable fraction of the AP III in muscle fibers were bound to myoplasmic constituents (Maylie et al., 1987) and if bound AP III did not react with calcium, both the amplitude of the AP III [Ca^{2+}] transients (Maylie et al., 1987 and Fig. 5, above) and the fura-2 K_D calculated therefrom as in Fig. 6 A and Table I would be larger than the values given here. As discussed in relation to Fig. 5, if two-thirds of the AP III in fibers were bound (Maylie et al., 1987) but in rapid equilibrium with unbound AP III, the AP III [Ca^{2+}] transient would be nine times larger than calculated assuming all AP III to be immediately available for reaction with calcium. In that case the K_D and resting values of [Ca^{2+}] would be nine times greater than the values reported in Table I. Interestingly, for the case of rapid equilibration of free and bound AP III the increase in K_D was produced entirely by a decrease in the value of k_{on}, with the value of k_{off} unchanged. For the case of irreversibly bound AP III the value of k_{off} was actually slightly less than that obtained assuming all AP III to be free and immediately available for reaction with [Ca^{2+}] (Fig. 5, legend). Thus the disagreement between values of k_{off} in fibers and in calibrating solutions cannot be attributed to an error in the scaling of the AP III [Ca^{2+}] transient due to the presence of bound AP III.

For the fits in Fig. 6 A and Table I, AP III was assumed to be in instantaneous equilibrium with [Ca^{2+}]. Slightly better fits of the theoretical to experimental fura-2 signals were obtained when the calcium-AP III reaction was assumed to be noninstantaneous. Previous comparison of simultaneous signals from AP III and azo-1 also indicated that the two signals could be better reconciled if AP III was assumed to react with [Ca^{2+}] with a slight kinetic delay (Baylor et al., 1985b). For the present calculations the dissociation constant for the calcium-AP III reaction was set at 17,500 μM^2 (Kovacs et al., 1983) and several different values were tried for the on rate constant of the reaction. The best fits were obtained with an on rate constant of 4×10^4 μM^{-2} s^{-1}. In this case both k_{on} and k_{off} for the Ca-fura-2 reaction were decreased (by $16 \pm 1\%$ and $11 \pm 2\%$, respectively, for the 18 fibers in Table I) and the mean value of K_D was slightly increased (by $6 \pm 1\%$) compared with when AP III was assumed to be in instantaneous equilibrium with [Ca^{2+}]. The values of $-R_{max}$ were the same whether or not AP III was assumed to be in instantaneous equilibrium with calcium. Because the correction for noninstantaneous reaction of AP III with calcium is somewhat arbitrary and relatively minor, we have used the fura-2 parameters obtained without correction for the AP III reaction kinetics.

The records in Fig. 6 B present the calcium transients obtained from the AP III absorbance signals (less noisy) superimposed on the calcium transients calculated from each of the corresponding fura-2 ratio signals (noisier) using Eq. 5 with the same parameter values as in Fig. 6 A. Near the peak of the calcium transients in Fig. 6 B the [Ca^{2+}] records calculated from the fura-2 signals are quite noisy, especially for the largest pulse (bottom). When the Ca-fura-2 reaction was near saturation, noise in the fura-2 ratio signal corresponded to relatively larger changes in free calcium than when fura-2 was far from saturation because the term $(R_{max} - R)$ in the denominator of Eq. 5 approached zero.

The vertical line crossing each pair of [Ca^{2+}] records in Fig. 5 B marks the identical point in time as the vertical line crossing the corresponding fura-2 fluorescence signals in Fig. 6 A. It marks the end of the interval used for the fit in Fig. 6 A. The records and vertical lines in Fig. 6 B show that by the end of the interval chosen for the fit, the AP III [Ca^{2+}] signal had fallen to close to its resting level. Thus the correction for an intrinsic signal (Kovacs and Schneider, 1977; Baylor et al., 1982b; Melzer et al., 1986a) and the possible presence of a small component due to slow changes in [Mg^{2+}] (Baylor et al., 1982a) in the AP III absorbance signal (Baylor et al., 1985a) would be relatively more important after the vertical line than earlier in the record. This may account for the divergence of experimental and theoretical fura-2 signals at late times in Fig. 6 A and justifies restriction of the fit interval to earlier times when these effects should have been less significant. If the fura-2 calibration parameters obtained during the fit interval are

valid, then the [Ca^{2+}] transient calculated from the fura-2 signal should be reliable both during and after the fit interval. At relatively late times the [Ca^{2+}] record calculated from the fura-2 signal should be even more reliable than that calculated from the AP III signal due to the absence of [Mg^{2+}] and intrinsic components from the fura-2 signal. Despite the differences in the measured and calculated fura-2 records after the fit interval in Fig. 6 A, the differences in the [Ca^{2+}] records calculated from the fura-2 and AP III signals are minimal both during and after the fit interval when the records are displayed on a scale appropriate for the full calcium transient as in Fig. 6 B.

Resting [Ca^{2+}] in Cut Muscle Fibers

The calibration of fura-2 in Table I provides the necessary parameters for calculating the resting level of [Ca^{2+}] from the values of $-R$ determined in those fibers at rest. The values obtained at $\sim$60 and 90 min after applying the dye-containing internal solution to the cut ends of the fibers are presented in the last two columns of Table I. The fibers were held at 0 mV during much of the first hour after dye application and were polarized to -100 mV about 5–10 min before determining the [Ca^{2+}] value for 1 h of dye exposure. The mean value of [Ca^{2+}] after 1 h of exposure to the dye containing internal solution was 49 ± 8 nM. Considering the presence of 100 μM EGTA and 50 μM fura-2 in the internal solution, both of which would tend to lower [Ca^{2+}], this value seems acceptably close to values of resting [Ca^{2+}] obtained in intact frog muscle fibers with calcium-sensitive microelectrodes (55 nM by Coray et al., 1980; 120 nM by Lopez et al., 1983). However, as discussed above, all calculated values of [Ca^{2+}] in Table I and elsewhere in this paper would have to

be increased if some of the AP III in the fiber were bound and unreactive with calcium when bound.

During the half hour after the first [Ca^{2+}] determinations in Table I various different pulse protocols were carried out on the fibers. At the end of this half hour the resting [Ca^{2+}] had increased in every fiber, on average to 101 ± 18 nM. A slow rise in resting [Ca^{2+}] during the course of the experiment was typical of all fibers studied. It usually became greatly accelerated just before fiber deterioration, which was indicated by a large increase in holding current often accompanied by swelling or contracture of the fiber.

The values of [Ca^{2+}] for the first four fibers in Table I were considerably lower than the values for the rest of the fibers in the table at both 60 and 90 min after exposure to dye. The last values of [Ca^{2+}] recorded in these fibers just before fiber deterioration (not presented in the table) were also lower than in the other fibers, suggesting a possible systematic underestimate of [Ca^{2+}] in these fibers.

Simultaneous High and Low Sensitivity Recording of [Ca^{2+}] Transients

The results in Fig. 6 indicate that self-consistent estimates of the complete time course of calcium transients in skeletal muscle fibers can be obtained by the combined application of AP III and fura-2, using AP III for the large and fast changes and fura-2 for the smaller, slower components. In Fig. 7 we apply this approach to study the effects of pulse duration on the [Ca^{2+}] transients. Fig. 7, A and B, present the same family of [Ca^{2+}] transients calculated from the AP III signals for pulses of 5–100 ms duration to -20 mV (bottom), but displayed on a relatively faster time scale in A than in B. Fig. 7, C and D, give fura-2 signals on
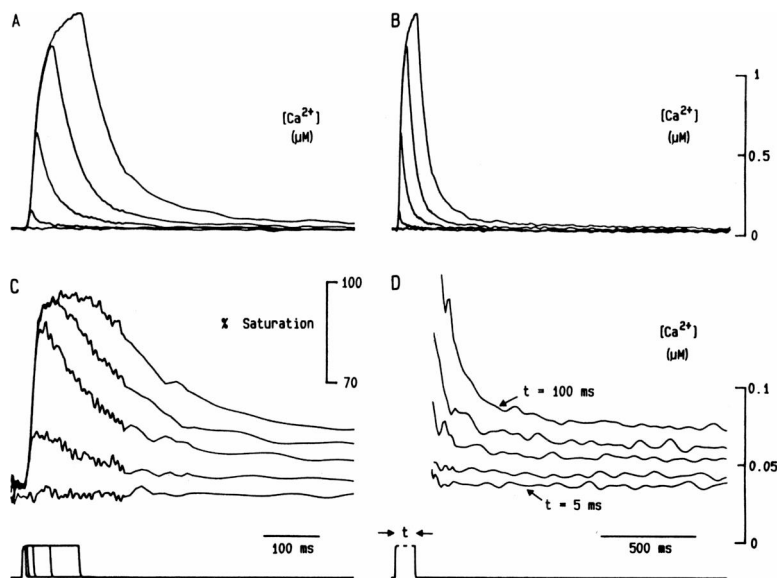
FIGURE 7 Calcium transients in a skeletal muscle fiber recorded simultaneously with antipyrylazo III and fura-2 for pulses of constant amplitude but varying duration. (A and B) [Ca^{2+}] records calculated from AP III absorbance signals at 700 nm. The same records are presented in A and B on different time scales. (C) Fura-2 percent saturation calculated from fura-2 fluorescence ratio signals recorded simultaneously with the AP III signals in A and B. Same time scale as in A. (D) [Ca^{2+}] records calculated from the fura-2 signals in C, presented on the same time scale as used for B. Because of the expanded [Ca^{2+}] axis used in D, the [Ca^{2+}] records were out of range during the pulses. When in range, the amplitudes of the "maintained" levels of [Ca^{2+}] after the pulses increased as the pulse duration (t, bottom) was increased from 5 to 100 ms. The values of the fura-2 constants obtained for this fiber as in Fig. 6 and used in C and D were $-R_{max} = -0.32$, $k_{on} = 3.65 \times 10^8$ M^{-1}s^{-1}, $k_{off} = 24$ s^{-1} ($-R_{min} = -2.00$, as in Fig. 6, legend). Fiber 370, 4.0 μm per sarcomere, 8.5°C, [AP III] 555–613 μM, fura-2 F_{358} increased by <5% during the sequence.

the same two time scales as used for the simultaneously recorded AP III calcium transients in Fig. 7, *A* and *B*, respectively. Fig. 7 *C* presents the fura-2 percent saturation signals, whereas Fig. 7 *D* shows the $[Ca^{2+}]$ signals calculated from the percent saturation using the fura-2 parameter values in the Fig. 7 legend. The vertical scale for the fura-2 $[Ca^{2+}]$ records (Fig. 7 *D*) is expanded 10-fold compared with the scale for the AP III $[Ca^{2+}]$ records in Fig. 7 *B* so as to emphasize small changes in $[Ca^{2+}]$ detected by fura-2. The fura-2 $[Ca^{2+}]$ records are thus off scale during and shortly after the pulses, when $[Ca^{2+}]$ was relatively high (Fig. 7 *B*). When they do come into range, the fura-2 $[Ca^{2+}]$ records show that there was a slowly decaying component of the calcium transient, the amplitude of which clearly increased with the duration of the preceding depolarizing pulse. The slow component was maintained for at least several seconds after fiber repolarization (Fig. 4 and other fibers not shown).

Effect of Holding Potential on Resting $[Ca^{2+}]$

The effects of steady partial depolarization on $[Ca^{2+}]$ were studied with fura-2 in a series of experiments using the "slow sampling" data acquisition routine (Methods). The average value of F_{380} was determined over a 1-s period and the determination was repeated every 5 s. Fluorescence ratio signals $(-R)$ were calculated for each F_{380} value using the F_{358} values monitored before and after the time interval over which the F_{380} values were obtained. $[Ca^{2+}]$ was calculated from each value of $-R$ using the mean values of K_D and $-R_{max}$ from Table I, with $-R_{min}$ as used for Table I. Relative to the time scale of the slow sampling records, fura-2 can be considered to be in equilibrium with $[Ca^{2+}]$ so that no correction was required for the fura-2 reaction kinetics and $[Ca^{2+}]$ was calculated from the fura-2 ratio signal according to Eq. 3.

The results of one experiment are presented in Fig. 8. For a 115-s depolarization from -100 to -65 mV, $[Ca^{2+}]$ rose slightly from 28 to 35 nM within 30 s and then remained roughly steady for the remainder of the depolarization. On repolarization to -100 mV $[Ca^{2+}]$ returned to close to its starting level. During the subsequent depolarization to -60 mV $[Ca^{2+}]$ rose to a peak of ~61 nM within 20 s and then continuously declined from this value during the remainder of the 150-s depolarization, approaching what appeared to be a steady level by the end of the depolarization. When the fiber was repolarized to -100 mV, $[Ca^{2+}]$ again returned to close to the level before depolarization. The changes in $[Ca^{2+}]$ in Fig. 8 recorded with fura-2 during voltage clamp depolarization of a frog cut skeletal muscle fiber are quite similar to aequorin light signals obtained from intact frog fibers injected with aequorin and subject to prolonged partial depolarization by changes in concentration of potassium in the external bathing solution (Snowdowne, 1985). It should be noted
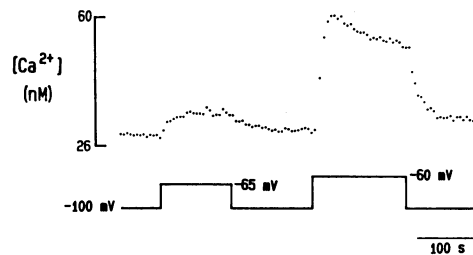

FIGURE 8 The influence of holding potential on intracellular $[Ca^{2+}]$. The fluorescence intensity at 380 nm excitation was recorded at 5-s intervals while the holding potential was changed. The fluorescence at 358 nm excitation was recorded ~30 s before and immediately after the squence shown. The ratio F_{380}/F_{358} was formed for each point by interpolating between the two F_{358} values. The $[Ca^{2+}]$ was calculated from the ratio with $-R_{max} = -0.34$, $-R_{min} = -1.91$, and $K_D = 89$ nM, the mean values from Table I. The upper panel shows the $[Ca^{2+}]$ as the membrane potential was changed from -100 mV to -65 and -60 mV (depicted schematically in the lower panel). Fiber 410, 4.0 μm per sarcomere, 9°C.

that the depolarizations used for Fig. 8 were sufficiently small that no change in $[Ca^{2+}]$ could be detected in the AP III absorbance signals using our present apparatus, whereas the fura-2 fluorescence provided clear evidence of changes in $[Ca^{2+}]$ for such depolarizations in this and several other fibers in which a protocol similar to that in Fig. 8 was used. The $[Ca^{2+}]$ levels in Fig. 8 were calculated using the fura-2 K_D obtained under the assumption that all AP III in a fiber is free and available for reaction with calcium, and would be higher if an appreciable fraction of the AP III were bound and not immediately available for reaction with calcium.

Effects of Fiber Movement on the AP III and Fura-2 Signals

Our standard procedure for using AP III to monitor $[Ca^{2+}]$ transients involves stretching fibers to remove any overlap of the thick and thin filaments and thus eliminate fiber movement and the related optical artifacts in the AP III signals. Occasionally fibers were not sufficiently stretched to eliminate all movement. Fig. 9 *A* presents records of relative changes in transmitted light intensity at 700 nm from one such fiber for pulses of 30 and 120 ms to -20 mV. The record for the longer pulse exhibits a definite movement artifact, as indicated by the bump in the falling phase of the record, in contrast to the smooth monotonic decay typical of 700 nm records from other fibers that did not exhibit movement. Direct observation confirmed the fiber movement for depolarizations of 60 and 120 ms. The records at 850 nm (not shown) recorded simultaneously with the 700 nm records in Fig. 9 *A* also exhibited a large movement artifact for the 120-ms pulse and indicated a smaller movement for the 30-ms pulse. In contrast, the fura-2 fluorescence signals recorded for the identical pulses and presented in Fig. 9 *C* exhibit no sign of any movement artifact for either the shorter or the longer pulse. The relative insensitivity of fluorescence signals to movement
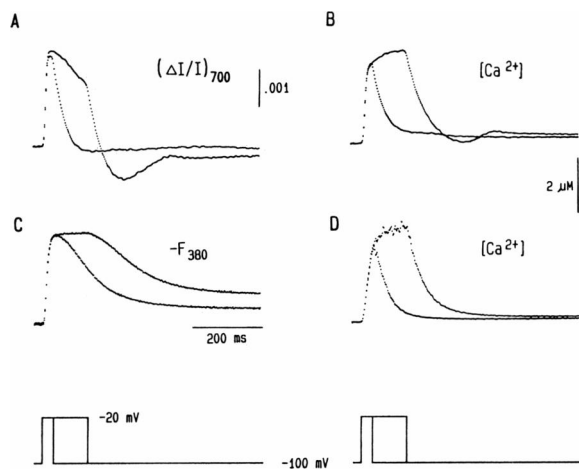
FIGURE 9 Relative insensitivity of fura-2 records to movement artifact. (A) $\Delta I/I$ records at 700 nm for 30- and 120-ms depolarizations to -20 mV in a fiber which exhibited movement. (B) Fluorescence signals for 380 nm excitation recorded simultaneously with the records shown in A. (C) $\Delta[Ca^{2+}]$ records calculated from the $\Delta I/I$ records in A after correction for intrinsic signals using $\Delta I/I$ at 850 nm (not shown). Note the remaining movement artifact on the signal corresponding to the 120-ms depolarization. (D) $[Ca^{2+}]$ records calculated from the fura-2 signals in B as described in text. Note the absence of a movement artifact. $k_{on} = 1.51 \times 10^8$ $M^{-1}s^{-1}$; $k_{off} = 25$ s^{-1}; $-R_{max} = -0.34$; and $-R_{min} = -1.91$. Fiber 416, 4.0 μm per sarcomere, 9°C.

artifacts compared to AP III absorbance signals arises directly from the relative changes represented by the two signals. The AP III signal represents only a fraction of a percent change in transmitted light intensity (Fig. 9 A) so that a fraction of a percent change in transmitted light due to fiber movement would produce an artifact that is as large as the entire AP III signal. In contrast, the fura-2 signal represents the total fluorescence of the fiber so that a given percent change in fluorescent light due to fiber movement would produce only the same percent artifact in the fura-2 signal. For example, in the fiber in Fig. 9 the movement artifact in the falling phase of the 700-nm record for the longer pulse appears to be roughly 0.1% of the incident light (Fig. 9 A). A similar 0.1% change in incident light intensity at 380 nm would have resulted in a 0.1% change in total fluorescence, which would be insignificant in the fura-2 record in Fig. 9 C.

Fig. 9 B shows the $[Ca^{2+}]$ transients calculated from the 700 nm (Fig. 9 A) and 850 nm (not shown) absorbance records in this fiber. The movement artifact is less severe in the $[Ca^{2+}]$ record than in the 700-nm absorbance record because the correction for the intrinsic signal also corrected some but not all of the movement artifact. If the wavelength dependence of the movement artifact had fortuitously been the same as the wavelength dependence of the intrinsic signal, the correction for intrinsic signal would have removed all of the movement artifact. Unfortunately, this is rarely the case.

Fig. 9 D presents $[Ca^{2+}]$ transients calculated from the fluorescence signals in Fig. 9 C. The values of $-R_{max}$, k_{on},

and k_{off} used to convert from fluorescence to $[Ca^{2+}]$ records were obtained from fits (not shown) similar to those in Fig. 6 using records for the two pulses in Fig. 9 and for one intermediate duration pulse not presented in Fig. 9. The fit interval was restricted to times before the start of obvious movement artifacts, as judged from the 850-nm absorbance records. The fura-2 $[Ca^{2+}]$ records in Fig. 9 D are very similar in amplitude and general time course to the AP III $[Ca^{2+}]$ transients in Fig. 9 B except that the movement artifact is undetectable in the fura-2 $[Ca^{2+}]$ records. This is not surprising because the raw 380-nm fluorescence records in Fig. 9 C themselves already lack the movement artifact. In this regard it is interesting to note that fura-2 may be potentially even more powerful in avoiding movement artifacts in $[Ca^{2+}]$ records than shown in Fig. 9. Even if a movement were sufficiently large to produce a definite artifact in the fluorescence record at 380 nm, much or all of this artifact might in principle be removed when taking the fluorescence ratio if the artifact arose from a change in the amount of fura-2 located in the excitation light beam, from a change in the intensity of illumination of the cell by the excitation beam or from a change in the fraction of the fluorescent light ultimately detected. However, to accomplish this, records would have to be obtained at both wavelengths for the same pulse with the identical fiber movement and the fluorescence ratio would have to be calculated point by point throughout the time course of the records.

DISCUSSION

The apparatus and procedures presented in this paper have allowed us to considerably extend the range of myoplasmic $[Ca^{2+}]$ changes that we can monitor compared with previous studies from this or other laboratories using AP III as the sole $[Ca^{2+}]$ indicator. This was achieved by using both AP III (relatively low affinity but rapid-reaction kinetics) and fura-2 (higher affinity but slower-reaction kinetics) simultaneously. Both dyes were added to the solutions bathing the cut ends of the fibers and entered the fibers by diffusion. Simultaneous use of the two indicators was possible with essentially no change in the elements of our previous optical system for AP III because fura-2 is a fluorescence indicator whereas AP III is an absorbance indicator and the wavelengths for fura-2 excitation and emission are well below the wavelengths that we use for monitoring the AP III absorbance signal. Light at four different wavelengths was used simultaneously for these measurements: 380 nm (fura-2 excitation), 510 nm (fura-2 emission), 700 nm (AP III absorbance) and 850 nm (intrinsic transparency signal). Light at all four wavelengths traversed a common path to (excitation) or from (emission, transmission) the fiber but was routed separately from its point of origin (excitation) or to its point of detection (emission, transmission) by three dichroic beam splitters of successively longer reflectance bands. Our use

of dichroic beam splitters of successively longer reflectance bands to split off signals of successively longer wavelengths from a beam of mixed wavelengths is patterned after a system recently described by Irving et al. (1987) for monitoring absorbance signals simultaneously at three different wavelengths. However, our implementation differs somewhat from theirs because we use one of the beam splitters to direct incident light toward the fiber (for fluorescence excitation) rather than to separate out a band of light leaving the fiber. Another difference is that we employed dichroic beam splitters rather than simple beam splitters. This maximized the fraction of light at each desired wavelength actually reaching each photodetector.

Our simultaneous recordings of AP III absorbance signals and fura-2 fluorescence signals (cf. Fig. 3) clearly illustrate the complementary advantages and disadvantages of these two Ca^{2+} indicators. The fura-2 signal is convenient for monitoring relatively small changes in $[Ca^{2+}]$ but inconvenient and, because of saturation, inappropriate for monitoring the relatively large $[Ca^{2+}]$ transients typical of skeletal muscle. In contrast, AP III is appropriate for monitoring the large $[Ca^{2+}]$ transients in muscle but is not sufficiently sensitive to reliably record changes in resting $[Ca^{2+}]$ or small elevations of myoplasmic $[Ca^{2+}]$ resulting from small depolarizations. The small residual elevations of $[Ca^{2+}]$ that follow the calcium transients for relatively large calcium releases can only be monitored by AP III with some uncertainty, whereas they can be unambiguously recorded with fura-2. The fura-2 signal is also much less sensitive than the AP III signal to artifacts due to fiber movement.

The simultaneous recordings of AP III and fura-2 signals also provided data for calibrating fura-2 in muscle fibers so as to be consistent with the AP III calcium transient. Using such calibrations the fura-2 fluorescence ratio signal can be corrected for kinetic delays in the Ca-fura-2 reaction. The corrected signal can then be used to calculate a calcium transient that is quantitatively similar to the simultaneously measured AP III calcium transient over the interval during which both could be reliably monitored. The combined use of the two indicators with the fura-2 calibration also allows the resting level of $[Ca^{2+}]$ from which the AP III calcium transient originates to be determined. This was not possible using AP III alone.

Our measurements with fura-2 indicated a gradual rise in resting $[Ca^{2+}]$ during the course of almost all experiments. A similar gradual rise in $[Ca^{2+}]$ might have caused the gradual widening of the calcium transient produced by an action potential during the course of the experiments of Maylie et al. (1987) on cut frog fibers under conditions very similar to ours. The widening could have been produced if increased resting $[Ca^{2+}]$ caused increased occupancy of slowly equilibrating myoplasmic calcium binding sites that contribute to the lowering of $[Ca^{2+}]$ after calcium release (Melzer et al., 1986a). In previous experi-

ments with AP III as the sole calcium indicator a slow rise in resting $[Ca^{2+}]$ could not have been detected.

The slow phase of decay seen in the present fura-2 signals (Figs. 4 and 7) provides the strongest evidence to date for a slow phase in the return of $[Ca^{2+}]$ to its resting level after calcium release. Previous studies using aequorin (Cannell, 1986) or AP III (Melzer et al., 1986a) have already indicated the existence of a small, slow component in the decay of $[Ca^{2+}]$ after calcium release. However, the aequorin signal is relatively insensitive to small changes in $[Ca^{2+}]$ because aequorin luminescence is proportional to $[Ca^{2+}]^{2.5}$ (Blinks et al., 1982). The small, slow component of the AP III 700-nm absorbance signal is strongly dependent on the correction for a simultaneous slow change in light transmission intrinsic to the fiber (Kovacs and Schneider, 1977; Baylor et al., 1982b; Melzer et al., 1986a) and may also be contaminated by a possible magnesium signal at 700 nm (Baylor et al., 1985a) due to prolonged elevation of $[Mg^{2+}]$ after calcium release (Baylor et al., 1982a). Because (a) the slow phase of the fura-2 signal does not appear to be appreciably contaminated by a magnesium signal (Fig. 4), (b) any intrinsic fluorescence signal is negligible compared with the measured fura-2 signal, and (c) changes in pH within the physiological range hardly affect the spectrum of either calcium-free or calcium-complexed fura-2 (Grynkiewicz et al., 1985), fura-2 appears to be the most reliable indicator available for monitoring the slow component in the decline of $[Ca^{2+}]$ after calcium release in skeletal muscle.

The actual concentration of fura-2 in a fiber was not needed for calculating $[Ca^{2+}]$ from the fura-2 ratio signal (Methods), but is of interest in terms of the possibilities that fura-2 may bind to myoplasmic constituents (Hollingworth and Baylor, 1987; Baylor and Hollingworth, 1987) or may be excluded from the myofilament lattice (Timmerman and Ashley, 1986). Our results show that in cut frog skeletal muscle fibers the equilibrium cytosolic concentration of free plus bound fura-2 was essentially equal to the concentration of fura-2 applied to the cut ends of the fiber. The simplest interpretation of this observation is that fura-2 is neither bound to cytosolic constituents nor excluded from the myofilament lattice. However, it is still possible that fura-2 is both bound and excluded, but that these two opposing effects were approximately equal so that the fura-2 content of the fibers was equal to the end pool concentration. Furthermore, the determination of fura-2 content of fibers depended on the as yet unverified assumption that the absolute absorbance and fluorescence efficiency of fura-2 for 358-nm excitation and 510-nm emission were the same in muscle fibers and in calibrating solution. However, the observation that the time course of dye entry was faster for fura-2 than for AP III in the same fiber suggests that the fractional binding of fura-2 was at least less than the fractional binding of AP III since the two dyes have similar molecular weights.

Comparison of the spectral properties of fura-2 in

resting and activated fibers with those of fura-2 in calibrating solutions revealed several differences. In muscle fibers the isosbestic wavelength was shorter, the values of $-F_{380}/F_{358}$ for calcium-free $(-R_{min})$ and calcium-complexed $(-R_{max})$ fura-2 were both more negative and the ratio of the fluorescence changes at 380–350 nm produced by changes in $[Ca^{2+}]$ were larger than in calibrating solutions. Some of these differences between fura-2 in solutions and in muscle fibers may be due to a more viscous environment in fibers than in solution, as suggested for fura-2 in PtK_1 cells (Poenie et al., 1986). Alternatively, some of the differences could be due to fura-2 binding in fibers, as indicated by fluorescence anisotropy measurements on intact fibers injected with fura-2 (Baylor and Hollingworth, 1987). The relatively slow reaction kinetics of fura-2 with calcium in fibers compared with solution might also result from fura-2 binding. In any case, the possibility of simultaneous recording with both fura-2 and AP III provides a means of calibrating the fura-2 reaction rate constants so as to obtain self-consistent calcium transients with the two indicators. Using this approach some uncertainty still remains regarding the absolute scale of the $[Ca^{2+}]$ signals. However, the uncertainty is the same for the $[Ca^{2+}]$ signals calculated for both the AP III (Maylie et al., 1987) and the fura-2 signals so that together the two signals do provide a means of monitoring relative changes in $[Ca^{2+}]$ over a wider range than could be practically achieved by either indicator alone.

APPENDIX

AP III absorbs light at both the excitation and emission wavelengths of fura-2. With simplifying assumptions regarding the fiber geometry and the optical set-up it is possible to derive a simple correction factor for the attenuation of the fura-2 signal by the presence of AP III.

It is assumed that the fiber cross-section can be approximated as a rectangle, and that the excitation and emission light travels through the fiber parallel to the optical axis of the microscope (Fig. 10). (A similar expression can be derived for an elliptical fiber but it requires a numerical integration.)

Denote the intensity of the incident excitation light entering the surface of the fiber by I_o, and the intensity of the emitted light leaving the fiber as I_{em}. From Beer's Law, the intensity of light, I, reaching the slab at a distance x from the top of the fiber is given by

$$I = I_0 10^{-(\epsilon_1 [D] x)}, \qquad (A1)$$

where $[D]$ is the concentration of AP III and ϵ_1 is the extinction coefficient of AP III at the incident wavelength. The fura-2 within the slab emits fluorescent light with intensity proportional to the incident light intensity, I, and the thickness of the slab, dx. As the light passes back through the fiber to the surface it is again absorbed by the AP III but now at the emitted wavelength. Again using Beer's Law, the emitted light from the slab at x reaching the surface, dI_{em}, is given by

$$dI_{em} = cI 10^{-(\epsilon_2 [D] x)} dx, \qquad (A2)$$

where c is a proportionality constant that depends on fura-2 concentration, fluorescence efficiency, and geometric factors, and ϵ_2 is the extinction coefficient of AP III at the emitted wavelength. Substituting Eq. A1
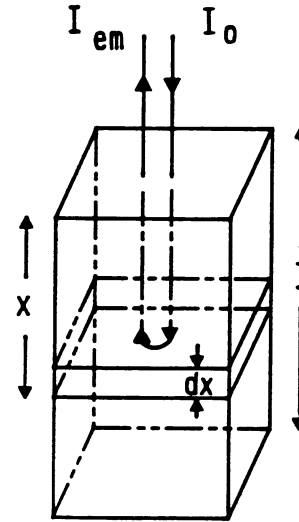

FIGURE 10 Schematic diagram of excitation and emission light paths used to calculate the correction to the fura-2 fluorescence due to light absorption by AP III.

into Eq. A2 and integrating over the fiber thickness along the optical axis gives

$$I_{em} = cI_0 \int_0^l 10^{-(\epsilon_1 [D] x)} dx$$

$$= cI_0 (1 - 10^{-(\epsilon_1 [D] l)})/(ln\ 10\ \epsilon_1 [D]\ l), \qquad (A3)$$

where $\epsilon_t = \epsilon_1 + \epsilon_2$ and l is the fiber thickness. Eq. A3 can be normalized (by dividing by I_{em} when $[D] = 0$) to obtain the fractional decrease in fura-2 emission as a function of the AP III dye concentration.

$$f = (1 - 10^{-A})/(ln\ 10\ A), \qquad (A4)$$

where $A = \epsilon_t D l$. To determine f from the actual absorbance measured during an experiment we can rewrite A as

$$A = aA_{550},$$

where $a = \epsilon_t/\epsilon_{550}$, ϵ_{550} is the extinction coefficient of AP III at 550 nm, and A_{550} is the measured absorbance at 550 nm due to the AP III in the fiber $(=\epsilon_{550} [D] l)$.

REFERENCES

Almers, W., and E. Neher. 1985. The Ca signal from fura-2 loaded mast cells depends strongly on the method of dye-loading. *FEBS (Fed. Eur. Biochem. Soc.) Lett.* 192:13–18.

Baylor, S. M., W. K. Chandler, and M. W. Marshall. 1982a. Optical measurements of intracellular pH and Mg^{++} in frog skeletal muscle fibres. *J. Physiol. (Lond.).* 331:105–138.

Baylor, S. M., W. K. Chandler, and M. W. Marshall. 1982b. Use of metallochromic dyes to measure changes in myoplasmic Ca^{++} during activity in frog skeletal muscle fibres. *J. Physiol. (Lond.).* 331:139–178.

Baylor, S. M., W. K. Chandler, and M. W. Marshall. 1983. Sarcoplasmic reticulum calcium release in frog skeletal muscle fibres estimated from arsenazo III calcium transients. J. Physiol. *(Lond.).* 331:625–666.

Baylor, S. M., and S. Hollingworth. 1987. Calcium transients in skeletal muscle fibers measured with indicator dyes. *J. Muscle Res. Cell Motil.* 8:461.

Baylor, S. M., M. E. Quinta-Ferreira, and C. S. Hui. 1985a. Isotropic components of antipyrylazo III signals from frog skeletal muscle fibers. *In* Calcium in Biological Systems. (R. P. Rubin, G. Weiss, and J. W. Putney, editors. Plenum Publishing Corp., New York. 339–349.

Baylor, S. M., S. Hollingworth, C. S. Hui, and M. E. Quinta-Ferreira. 1985b. Calcium transients from intact frog skeletal muscle fibres simultaneously injected with antipyrylazo III and azo 1. *J. Physiol. (Lond.).* 365:70.

Baylor, S. M., S. Hollingworth, C. S. Hui, and M. E. Quinta-Ferreira. 1986. Properties of the metallochromic dyes arsenazo III, antipyrylazo III and azo 1 in frog skeletal muscle fibres at rest. *J. Physiol. (Lond.).* 377:89–141.

Blinks, J. R., R. Rudel, and S. R. Taylor. 1978. Calcium transients in isolated amphibian skeletal muscle fibres: detection with aequorin. *J. Physiol. (Lond.).* 277:291–323.

Blinks, J. R., W. G. Wier, P. Hess and F. G. Prendergast. 1982. Measurement of Ca^{2+} concentrations in living cells. *Progr. Biophys. Mol. Biol.* 40:1–114.

Brum, G., E. Rios, and M. F. Schneider. 1988. A quantitative model of calcium removal from the myoplasmic solution. *J. Physiol. (Lond.).* 398:467–471.

Cannell, M. B. 1986. Effect of tetanus duration on the free calcium during the relaxation of frog skeletal muscle fiber. *J. Physiol. (Lond.).* 376:203–218.

Cannell, M. B., and D. G. Allen. 1984. Model of calcium movements during activation in the sarcomere of frog skeletal muscle. *Biophys. J.* 45:913–925.

Cleland, W. W. 1967. The statistical analysis of enzyme kinetic data. *Adv. Enzymol.* 29:1–32.

Coray, A., C. H. Fry, P. Hess, J. A. S. McGuigan, and R. Weingart. 1980. Resting calcium in sheep cardiac tissue and in frog skeletal muscle measured with ion-selective micro-electrodes. *J. Physiol.* 305:60–61.

Grynkiewicz, G., M. Poenie, and R. Y. Tsien. 1985. A new generation of Ca^{2+} indicators with greatly improved fluorescence properties. *J. Biol. Chem.* 260:3440–3450.

Hill, A. V., and J. V. Howarth. 1957. The effect of potassium on the resting metabolism of frog's sartorius. *Proc. R. Soc. Lond. B Biol Sci.* 147:21–43.

Hollingworth, S., and S. M. Baylor. 1987. Fura-2 signals from intact frog skeletal muscle fibers. *Biophys. J.* 51:549a.

Hollingworth, S., R. W. Aldrich, and S. M. Baylor. 1987. In vitro calibration of the equilibrium reactions of the metalochromic indicator dye antipyrylazo III with calcium. *Biophys. J.* 51:383–393.

Irving, M., J. Maylie, N. L. Sizto, and W. K. Chandler. 1987. Intrinsic optical and passive electrical properties of cut frog twitch fibers. *J. Gen. Physiol.* 89:1–40.

Jackson, A. P., M. P. Timmerman, C. R. Bagshaw, and C. C. Ashley. 1987. The kinetics of calcium binding to fura-2 and indo-1. FEBS (Fed. Eur. Biochem. Soc.) Lett. 216:35–39.

Klein, M. G., B. J. Simon, G. Szucs, and M. F. Schneider. 1987. Myoplasmic calcium transients monitored simultaneously with high and low affinity calcium indicators. *Biophys. J.* 51:199a.

Kovacs, L., and M. F. Schneider. 1977. An increase in optical transparency associated with excitation-contraction coupling in voltage-clamped cut skeletal muscle fibers. *Nature (Lond.).* 265:556–560.

Kovacs, L., Rios, E., and M. F. Schneider. 1983. Measurement and modification of free calcium transients in frog skeletal muscle fibres by a metallochromic indicator dye. *J. Physiol.* 343:161–196.

Kress, M., H. E. Huxley, A. R. Faruqi, and J. Hendrix. 1986. Structural changes during activation of frog muscle studied by time-resolved X-ray diffraction. *J. Mol. Biol.* 188:325–342.

Lopez, J. R., R. L. Alamo, C. Caputo, R. DiPolo, and J. Vergara. 1983. Determination of ionic calcium in frog skeletal muscle fibers. *Biophys. J.* 43:1–4.

Malencik, D. A., and E. H. Fischer. 1982. Structure, function and regulation of phosphorylase kinase. *In* Calcium and Cell Function. W. Y. Cheung, editor. Academic Press, New York. 161–188.

Maylie, J., M. Irving, N. L. Sizto, and W. K. Chandler. 1987. Calcium signals recorded from cut frog twitch fibers containing antipyrylazo III. *J. Gen. Physiol.* 89:83–143.

Melzer, W., E. Rios, and M. F. Schneider. 1984. The course of calcium release and removal in skeletal muscle fibers. *Biophys. J.* 45:637–641.

Melzer W., E. Rios, and M. F. Schneider. 1986a. The removal of myoplasmic free calcium following calcium release in frog skeletal muscle. *J. Physiol.* 372:261–292.

Melzer, W., M. F. Schneider, B. J. Simon, and G. Szucs. 1986b. Intramembrane change movement and calcium release in frog skeletal muscle. *J. Physiol.* 373:481–511.

Melzer, W., E. Rios, and M. F. Schneider. 1987. A general procedure for determining calcium release from the sarcoplasmic reticulum in skeletal muscle fibers. *Biophys. J.* 51:849–863.

Miledi, R., I. Parker, and G. Schalow. 1977. Measurement of calcium transients in frog muscle by the use of arsenazo III. *Proc. R. Soc. Lond. B Biol. Sci.* 198:201–210.

Poenie, M., J. Alderton, R. Steinhardt, and R. Tsien. 1986. Calcium rises abruptly and briefly throughout the cell at the onset of anaphase. *Science (Wash. DC).* 233:886–889.

Ratzlaff, K. L. 1987. Introduction to Computer-Assisted Experimentation. John Wiley & Sons, New York. 438 pp.

Rios, E., and M. F. Schneider. 1981. Stoichiometry of the reactions of calcium with the metallochromic indicator dye Antipyrylazo III and Arsenzo III. *Biophys. J.* 36:607–621.

Scarborough, J. B., 1966. Numerical Mathematical Analysis. Johns Hopkins Press, Baltimore.

Scarpa, A., F. J. Brinley, and G. Dubyak. 1978. Antipyrylazo III, a "middle range" Ca^{2+} metallochromic indicator. *Biochemistry.* 17:1378–1386.

Schneider, M. F., B. J. Simon, and G. Szucs. 1987a. Depletion of calcium from the sarcoplasmic reticulum during calcium release in frog skeletal muscle. *J. Physiol.* 392:167–192.

Schneider, M. F., B. J. Simon, G. Szucs, and M. G. Klein. 1987b. Calcium movement in skeletal muscle: measurement with antipyrylazo III and fura-2. *J. Muscle Res. Cell Motil.* 8:461–462.

Simon, B. J., M. F. Schneider, and G. Szucs. 1985. Inactivation of sarcoplasmic reticulum calcium release in frog skeletal muscle is mediated by calcium *J. Gen. Physiol.* 86:36a.

Smith, C. G., and D. Y. Solandt. 1938. The relation of contracture to the increment in the resting heat production of muscle under the influence of potassium. *J. Physiol.* 93:305–311.

Snowdowne, K. W., 1985. Subcontracture depolarizations increase sarcoplasmic ionized calcium in frog skeletal muscle. *Am. J. Physiol.* 248:C520–C526.

Solandt, D. Y. 1938. The effect of potassium on the excitability and resting metabolism of frog's muscle. *J. Physiol.* 86:162–170.

Zot, H. G., and J. D. Potter. 1984. The role of calcium in the regulation of the skeletal muscle contraction-relaxation cycle. *In* Metal Ions in Biological Systems. Calcium and Its Role in Biology. (H. Siegel, ed.), Marcel Decker, New York. 17:381–410.